

NOTE TO USERS

This reproduction is the best copy available.

UMI[®]

01566966x

ADAPTIVE POWER LINE HARMONIC DETECTION FOR ACTIVE FILTER APPLICATIONS

By

WEIDONG LIU

(MEng, Northeastern University, China, 1991)

(BSc, Northeastern University, China, 1988)

A thesis

presented to Ryerson University
in partial fulfillment of the
requirements for the degree of
Master of Applied Science
in the Program of
Electrical and Computer Engineering

Toronto, Ontario, Canada, 2004

© WEIDONG LIU 2004

PROPERTY OF
RYERSON UNIVERSITY LIBRARY

UMI Number: EC52961

INFORMATION TO USERS

The quality of this reproduction is dependent upon the quality of the copy submitted. Broken or indistinct print, colored or poor quality illustrations and photographs, print bleed-through, substandard margins, and improper alignment can adversely affect reproduction.

In the unlikely event that the author did not send a complete manuscript and there are missing pages, these will be noted. Also, if unauthorized copyright material had to be removed, a note will indicate the deletion.

UMI[®]

UMI Microform EC52961

Copyright 2008 by ProQuest LLC.

All rights reserved. This microform edition is protected against unauthorized copying under Title 17, United States Code.

ProQuest LLC
789 E. Eisenhower Parkway
PO Box 1346
Ann Arbor, MI 48106-1346

Abstract

Adaptive Power Line Harmonic Detection For Active Filter Applications

WEIDONG LIU

Master of Applied Science of Electrical and Computer Engineering
Ryerson University, Toronto, 2004

The objective of this thesis research is to develop an efficient method for accurate detections of power line harmonic distortions for the control of active filters. The research has achieved its objective with four significant results. First, *an adaptive power line harmonic detection method* is developed, which is based on the findings of extensive research in the areas of inside and outside of power electronics controls. Second, *a simple and practical formulation of the adaptive harmonic detection method* is developed, which is simplified significantly from the original complex design formulations for noise cancellations. Third, *vigorous verifications of effectiveness of the adaptive detection method using computer simulations* are carried out, which cover the steady state operations, the dynamic operations, normal power line conditions, non-ideal supply and load conditions, etc. Fourth, *experimental verifications of the accuracy of the adaptive detection method* are conducted, which cover typical distorted power line conditions for normal and unbalanced operations. For illustration, this thesis presents carefully designed computer simulation and experimental case studies that cover a wide range of power line conditions.

Acknowledgement

The author wishes to express his deep gratitude to his supervisor Professor R. W. Y. Cheung for his expert supervision. The author highly appreciates the valuable advices, guidance, and encouragement from Professor Cheung through this thesis research.

The author also wishes to thank Professor B. Wu for his great help and support.

The author would like to convey the warmest thanks to his family and friends, especially Wade, for their support and encouragement.

Contents

1	Introduction	1
1.1	Background of active power line filtering operations	1
1.2	Introduction of contents in this thesis	3
2	Power Line Harmonics Control Methods	6
2.1	Basic concept of active power line filtering	7
2.2	Conventional detection methods for active filters	9
2.2.1	Instantaneous reactive power detection	11
2.2.2	Synchronous detection	14
2.3	Concept of adaptive noise detection	15
2.4	Concluding remarks	18
3	Adaptive Harmonic Detection Method for Active Filter Controls	20
3.1	Adaptive harmonic detection algorithm	21
3.2	Application of adaptive noise cancellation algorithm for harmonic detection	27
3.3	Uncorrelationship between u and i_{comp} and between i_a and i_{comp}	29
3.4	Simulink model for adaptive noise cancelling algorithm	31
3.5	Concluding Remarks	32
4	Effectiveness of Adaptive Harmonic Detection Method for Control of Active Filter	33
4.1	Verification using a square wave with known harmonic distortion	35
4.1.1	Square wave in phase with reference signal	35
4.1.2	Square wave and reference signal not in phase	36
4.1.3	Square wave with changing amplitude	37
4.1.4	Performances study with different values of performance factor μ	37
4.2	Modeling of power electronic loads for active filtering study	38
4.2.1	Rectifier with RL load as harmonic source on power line	39

4.2.2	Rectifier with RLC load with higher harmonic injection on power line	40
4.2.3	Unbalanced load as a combination of rectifier and single-phase loads	40
4.3	Verification of adaptive harmonic detection method for steady state operations	41
4.3.1	Harmonics from rectifier RL load with normal or unbalanced line voltage	42
4.3.2	Harmonics from rectifier RLC load with unbalanced line voltage	44
4.3.3	Harmonics from rectifier load with unbalanced single-phase loads	46
4.4	Verification of adaptive harmonic detection method for dynamic operation	47
4.5	Comparison with conventional detection methods	48
4.5.1	Comparison under normal power line voltage	49
4.5.2	Comparison for unbalanced power line voltage condition	50
4.6	Concluding remarks	52
5	Experimental Verification of Adaptive Harmonic Detection Method	53
5.1	Hardware DSP implementation of adaptive harmonic detection	54
5.1.1	Digital Signal Processor Control Circuit	54
5.1.2	Active filter power circuit	58
5.2	Software DSP implementation of adaptive harmonic detection	59
5.2.1	Software setting for analog-to-digital conversion	59
5.2.2	Computation of fundamental power line current	60
5.2.3	Updating weights for adaptive harmonic detection	61
5.2.4	PWM generation	62
5.2.5	Flow chart for DSP software control	64
5.3	Experimental verification of the adaptive harmonic detection method	66
5.3.1	RL rectifier load (Case study 1: moderate power line harmonics)	66
5.3.2	RLC rectifier load (Case study 2: more power line harmonics)	68
5.3.3	RC rectifier load (Case study 3: increased power line harmonics)	70
5.3.4	Unbalanced distorted load (Case study 4: unbalanced power line harmonics)	72
5.4	Concluding remarks	74

6 Conclusion	76
6.1 Major research work completed	76
6.2 Major research contributions	78
6.3 Future work	78
Bibliography	80
Appendix A Simulation Models for Two Conventional Detection Methods	85
Appendix B Simulation Results of Two Conventional Detection Methods	87
Appendix C DSP Software Codes for Adaptive Harmonic Detection Method	93

List of Figures

Figure 2.1	A simple circuit block diagram for illustration of active filtering	8
Figure 2.2	α - β coordinates transformation	12
Figure 2.3	Block diagram for adaptive noise cancellation	16
Figure 3.1	adaptive linear combiner	21
Figure 3.2	The adaptive compensator	25
Figure 3.3	Application of adaptive noise cancellation for power line harmonic detection	28
Figure 3.4	Model of adaptive noise cancelling algorithm	31
Figure 4.1	Verification of harmonic detection using a square wave	36
Figure 4.2	(a) In-phase fundamental component (b) total harmonic plus out-of-phase fundamental component	36
Figure 4.3	Harmonic detection of a square wave with changing amplitude	37
Figure 4.4	Output of the adaptive filter with $\mu = 2 \times 10^{-5}$	38
Figure 4.5	Output of the adaptive filter with $\mu = 10^{-4}$	38
Figure 4.6	Active filtering of harmonics generated by rectifier with RL load	40
Figure 4.7	Active filtering of harmonics generated by rectifier with RLC load	40
Figure 4.8	Active filtering of harmonics generated by unbalanced nonlinear loads	41
Figure 4.9	Detection for rectifier RL load under normal line voltage	42
Figure 4.10	Detection for rectifier RL load under unbalanced line voltage	44
Figure 4.11	Detection for rectifier RLC load with non-ideal line voltage	45
Figure 4.12	Detection for three unequal single-phase loads and a rectifier load	46
Figure 4.13	load current with changing amplitude	48
Figure 5.1	Block diagram of the active filter	55
Figure 5.2	Block diagram of DSP TM320LF2407	57
Figure 5.3	Block diagram of the software	59
Figure 5.4	Diagram of buffer at step n and step n+1	61
Figure 5.5	DSP connections to the inverter of the active filter	64
Figure 5.6	Flow chart for the adaptive control of active filter	65
Figure 5.7	Experimental results for Case Study 1	67

Figure 5.8	Simulation results for Case Study 1	68
Figure 5.9	Experimental results for Case study 2	69
Figure 5.10	Simulation results for Case study 2	70
Figure 5.11	Experimental results for Case study 3	71
Figure 5.12	Simulation results for Case study 3	72
Figure 5.13	Experiment results for Case study 4	73
Figure 5.14	Simulation results for Case study 4	74
Figure A1	Model of instantaneous reactive power method	86
Figure A2	Model of synchronous detection method	86
Figure B1	Detection results of rectifier RL load using instantaneous reactive power method	87
Figure B2	Detection results of rectifier RL load using synchronous detection method	88
Figure B3	Detection results of unbalanced load using instantaneous reactive power method	88
Figure B4	Detection results of unbalanced load using synchronous detection method	89
Figure B5	Detection results of rectifier RL load using instantaneous reactive power method with unbalanced power line voltage	90
Figure B6	Detection results of rectifier RL load using synchronous detection method with unbalanced power line voltage	90
Figure B7	Detection results of rectifier RLC load using instantaneous reactive power method with unbalanced power line voltage	91
Figure B8	Detection results of rectifier RLC load using synchronous detection method with unbalanced power line voltage	92

List of Tables

Table 4.1:	THD (%) for the waveforms in Figure 4.9	43
Table 4.2:	THD (%) for the waveforms in Figure 4.10	44
Table 4.3:	THD (%) for the waveforms in Figure 4.11	46
Table 4.4:	THD (%) for waveforms in Figure 4.12	47
Table 4.5:	THD (%) of line current under rectifier RL load for three detection methods	49
Table 4.6:	THD (%) of line current under unbalanced load for three methods	50
Table 4.7:	THD (%) of rectifier RL load with unbalanced power line voltage	51
Table 4.8:	THD (%) of rectifier RLC load with unbalanced power line voltage	51

Chapter 1

Introduction

Ideally the electrical supply voltage should be a sine wave of 60 Hz in North America. However, the voltage of some power supplies may considerably depart from the ideal condition due to disturbances on the power line system feeding these supplies. The disturbances may be caused by the nature such as lightning or by non-linear loads such as large power electronic equipment, for example high power electric drives [1-3]. The naturally occurred disturbances are usually transients that can be suppressed by protective devices such as surge arresters, and these disturbances usually last for a short duration. On the other hand, the disturbances caused by non-linear loads will stay in the supply system as long as the non-linear loads are operating. These disturbances can cause abnormal operations of neighboring equipment or even damage them. Also the disturbances can affect the operation of the equipment that originally creates the disturbances. An objective of this thesis research is to investigate methods for elimination of these disturbances on the power line.

1.1 Background of Active Power Line Filtering Operations

This thesis research has found that active power filter can effectively eliminate the harmonic disturbances caused by non-linear loads on the power line. An active filter is basically a power electronic inverter that, if operates properly, can inject *equal-but-opposite* amount of compensating harmonics into the power line to cancel the original harmonics [1, 5, 8]. The focus of this thesis research is to increase the harmonics elimination capability of active

power line filters by improving the accuracy of their harmonic detection ability particularly for real (non-ideal) industrial systems.

An active filter circuit basically consists of the power inverter circuit and a control circuit. The common operation of the active filter is: first the harmonic-detecting unit in the control circuit samples the instantaneous waveform of the power-line voltage and current and then computes the required compensation current. Second, based on the computed compensation current, the control unit generates firing signals to drive the inverter circuit. Third, according to the firing sequence, the inverter generates the compensating currents and injects them into the power line to cancel its harmonic distortion. This thesis will detail the hardware and software implementation of the power circuit and the control circuit of the active power line filter.

The concept for the active power filter operation is straight forward that involves two basic steps: measuring the harmonics in the power line, and driving the inverter to cancel them. In practice, however, it is difficult to eliminate all harmonics in the power line completely. One major difficulty found in this thesis research is the inaccurate detection of changing power line harmonics by the conventional detecting methods, due to the interaction of the active filter and the power electronic equipment that generates the original harmonics. This thesis research has developed an accurate, adaptive harmonic detection method for active filter applications.

Harmonic detection is a very important step for the compensation of power line harmonics. If harmonics are not detected accurately, the power line can be either under-compensated or over-compensated.

Conventionally, harmonics have been detected and controlled by using frequency-domain compensating method and time-domain compensating method. There have been many methods proposed for the detection of harmonics in both frequency-domain and time-domain [6-8]. However, the applications of the existing methods are very limited because of the restrictions and assumptions made during the development of the theory. Therefore, their performances vary depending on the mains conditions and power electronic loads. Some methods work well only when the mains voltage is in ideal condition. Others can only deal with certain types of power electronic loads.

In this thesis, an adaptive harmonic detection method is developed to overcome the above-mentioned problems. This method adapts very well to the changes of loading and line conditions and provides accurate detections of the power line current distortions.

1.2 Introduction of Contents in This Thesis

The following provides an introduction of the chapters in this thesis.

Chapter 2 presents the concept and methods for the control of power-line harmonics using active filters. The focus of this chapter is first to discuss the research findings on state-of-the-art active filtering control methods, and second to present a novel approach for active filter control based on adaptive noise cancellation theory. This theory, which was originally developed for noise signal processing, is applied by this thesis research for the control of the power line active filter. This chapter presents the conventional harmonic detection methods, both in

frequency domain and in time domain. Also this chapter identifies areas of insufficiency for the conventional methods.

Chapter 3 presents the adaptive harmonic detection method for the control of active filters. The focus of this chapter is to detail the adaptive harmonic detection algorithm, and to apply this algorithm for the active filter control. The adaptive harmonic detection algorithm is developed based on the theory of adaptive noise cancellation.

Chapter 4 first presents a vigorous verification of the adaptive harmonic detection method using a square wave current of known harmonic distortion. Second, this chapter verifies the effectiveness of the adaptive detection method for steady state operations under typical power line conditions including line distortion caused by rectifier carrying different loads. Third, this chapter verifies the performance of the adaptive detection method for a dynamic operation where two additional rectifier loads are switched in. Fourth, this chapter demonstrates that the adaptive detection method performs better than two well-known conventional detection methods particularly under abnormal power line conditions.

Chapter 5 provides the experimental verification of the adaptive harmonic detection method for the control of active power line filters. This chapter demonstrates that the adaptive method is successfully implemented using state-of-the-art digital signal processor (DSP). This chapter presents the details of the hardware and the software implementations of the adaptive harmonic detection control. This chapter also presents four case studies: three for typical distorted power line

conditions, and one for unbalanced power line condition. The objective of these case studies is to demonstrate the effectiveness of the adaptive harmonic detection method for both balanced and unbalanced distorted power line conditions. Experimental results and simulations are provided for the demonstration.

Chapter 6 presents the conclusion of this thesis research and the future work in active power line filter controls.

Chapter 2

Power Line Harmonics Control Methods

This chapter presents the concept and methods for the control of power-line harmonics using active filters. The focus of this chapter is first to discuss the research findings on state-of-the-art active filtering control methods, and second to present a novel approach for active filter control based on adaptive noise cancellation theory. This theory, which was originally developed for noise signal processing, is applied by this thesis research for the control of the power line active filter. The following lists the sections in this chapter:

Section 2.1 presents the concept of active power line filtering. This section provides the basic operation principle, circuit connection, and compensating formulation.

Section 2.2 reviews the conventional harmonic detection methods used in the control of active filters. This section presents the key formulations for typical conventional methods, and analyzes the areas of insufficiency that concludes the need of an improved harmonic detection method.

Section 2.3 presents the concept of an adaptive noise cancellation method, based on which an effective harmonic detection method is developed in this thesis research for the power line active filtering applications. This section provides the key information for the adaptive noise cancellation operation.

Section 2.4 provides the concluding remarks for this chapter.

2.1 Basic Concept of Active Power Line Filtering

The basic concept of active power line filtering was introduced in [1]. Active filtering simply uses a power electronic inverter to inject *equal-but-opposite* amount of harmonics into the power line to cancel the original ones. This concept has been widely accepted and the research activities on active filtering have been increasing rapidly. A typical active filter circuit is composed of a power circuit and a control circuit. The power circuit is commonly a standard inverter of three-phase bridge configuration with *six* power electronic switches for the industrial *three*-phase systems, or with *four* switches for the *single*-phase systems. The control circuit, in general, has a harmonics detecting unit, a filter processing unit, and a inverter firing unit. The active filter control circuit first samples the instantaneous waveforms of the power-line voltage and current, and then determines the waveform of the compensating current required for elimination of the line harmonics. Based on the computed compensating waveform, the control circuit generates switching signals to the inverter. The inverter then injects the compensating current into the power line to cancel its harmonics. This thesis develops a novel method for the detection of power line harmonic distortion.

The basic operation principle of active filter can be illustrated using Figure 2.1 [2]. In this figure, u_s is the utility voltage source, L_s is the source impedance including the power line impedance, i_s is the supply current, v_t is supply voltage, i_c is the compensating current, i_L is the load current, and CT is the current transformer or transducer. The non-linear load generates harmonics on the power line, and the active filter injects counter-harmonics to cancel them.

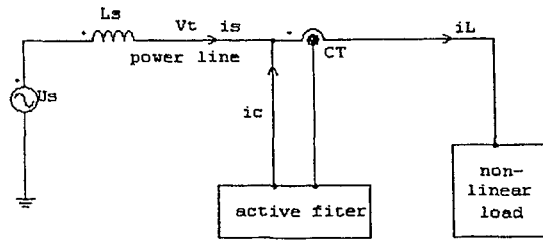


Figure 2.1: A simple circuit block diagram for illustration of active filtering

The utility source voltage u_s is originally sinusoidal, but the voltage on the power line v_t becomes distorted when supplying non-linear loads, particularly large power electronic equipment such as electric motor drives. These voltages can be expressed as:

$$\begin{aligned} u_s(t) &= U_s \sin \omega t \\ v_t(t) &= u_s(t) + f(i_L(t)) \end{aligned} \quad (2.1.1)$$

The distortion of the power line voltage v_t is a function of the load current. The non-linear load draws non-sinusoidal current that can be resolved into harmonic components using Fourier transformation. The load current can then be written as:

$$\begin{aligned} i_L(t) &= I_1 \sin(\omega t + \varphi_1) + \sum_{n=2}^{\infty} I_n \sin(n\omega t + \varphi_n) \\ &= i_1(t) + i_h(t) \end{aligned} \quad (2.1.2)$$

where i_1 is the fundamental current component and i_h is the summation of the high-order harmonic current components. The fundamental component i_1 can be further decomposed into two parts:

$$i_1(t) = i_s(t) + i_q(t) \quad (2.1.3)$$

where i_s is the active current component which has the same frequency (60 Hz) and in phase with the source voltage u_s , and i_q is the reactive current component which is 90 degrees out-of-phase of i_s . Equation (2.1.2) can be rewritten as:

$$\begin{aligned}
i_L(t) &= i_1(t) + i_h(t) \\
&= i_s(t) + i_q(t) + i_h(t) \\
&= i_s(t) + i_{comp}(t)
\end{aligned}
\tag{2.1.4}$$

where i_{comp} is the current needed to be compensated by the active filter.

As shown Figure 2.1, the active filter measures the current i_L of the non-linear load through a current transducer. The active filter processes this current and decomposes it into two: one is the required compensating current i_{comp} to be generated from the active filter, and the other is the resulting non-distorted current i_s to be supplied by the utility source.

2.2 Conventional Detection Methods For Active Filters

Harmonic detection is very crucial to the control of active filters. If harmonics in the power line are not detected accurately, the active filter cannot effectively cancel or suppress the harmonic distortion caused by the non-linear loads. Under this condition, the active filter will inject whatever harmonic current left from the harmonic cancelling operation into the power line. Therefore, this thesis is focused on the development of an effective method for power line harmonic detections. In this section, however, the conventional detection methods are presented, key formulations are given, and areas of insufficiency are discussed that concludes the need of an improved harmonic detection method.

There are two commonly used groups of control methods for active filters, namely the frequency-domain compensating methods and the time-domain compensating methods [3]. They are described in the following.

Frequency-domain detection:

Frequency-domain methods perform Fourier transformation on the measurements of the distorted power line current to obtain the harmonic contents and then to determine the amount and waveform of the compensating current. These methods utilize the periodicity of the distorted waveform to produce the compensating output. They are not effective for non-periodic power line distortions, but the non-periodic distortions are often found in the industrial sites. Another drawback of the frequency-domain method is that the Fourier transformation needs a lot of computations and thus is not time-efficient for real time control.

In general, frequency-domain methods are useful when the power line has a few low-order harmonics and their magnitudes change slowly. However, if the power line has a considerable amount of high-order, fast-changing harmonics, then the determination of the harmonics must require a lot of small-step calculations to produce accurate compensating signals for driving the active filter.

Time-domain detection:

Time-domain compensating methods are based on the instantaneous measurements of the distorted power line voltage and current to compute the compensating signals. In principle, these methods can compensate both periodic and non-periodic power line distortions [11-23].

Many harmonic detection methods in time domain have been reported [3,4]. The typical ones are: instantaneous reactive power method [5], synchronous detection method [6], flux-based controller [7], and notch filter method [8], etc. The effectiveness of these methods

varies depending on the assumptions used. Some methods assume the three-phase power supply to be balance, the supply voltages to be near perfect sinusoidal, etc. Thus, their applications are limited. The instantaneous reactive power method and the synchronous detection method are introduced in the following sections, because these methods are widely used and often appear in the literatures and also they will be used to compare with the method developed in this thesis.

2.2.1 Instantaneous Reactive Power Detection

The instantaneous reactive power transformation method was proposed by Akagi, et. Al. [5]. This method uses a matrix to map the three-phase supply voltage and current into instantaneous power-based space vector. First, the three-phase voltage and current are expressed as instantaneous space vectors in the a - b - c coordinates. The a , b , and c axes are fixed on the same plane, apart from each other by $2\pi/3$ radians, as shown in Figure 2.2. e_a , e_b , and e_c , are voltages, and i_a , i_b , and i_c , are currents. Second, these vectors can be transformed into a two-axis, α - β coordinates by using the following matrix:

$$\begin{bmatrix} e_\alpha \\ e_\beta \end{bmatrix} = \sqrt{\frac{2}{3}} \begin{bmatrix} 1 & -\frac{1}{2} & -\frac{1}{2} \\ 0 & \frac{\sqrt{3}}{2} & -\frac{\sqrt{3}}{2} \end{bmatrix} \begin{bmatrix} e_a \\ e_b \\ e_c \end{bmatrix} \quad (2.2.1)$$

$$\begin{bmatrix} i_\alpha \\ i_\beta \end{bmatrix} = \sqrt{\frac{2}{3}} \begin{bmatrix} 1 & -\frac{1}{2} & -\frac{1}{2} \\ 0 & \frac{\sqrt{3}}{2} & -\frac{\sqrt{3}}{2} \end{bmatrix} \begin{bmatrix} i_a \\ i_b \\ i_c \end{bmatrix} \quad (2.2.2)$$

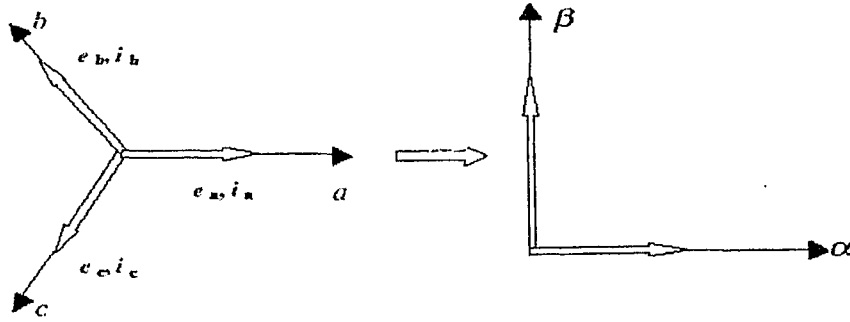


Figure 2.2: α - β coordinates transformation.

The instantaneous power can be expressed as:

$$p = e_\alpha * i_\alpha + e_\beta * i_\beta = e_a i_a + e_b i_b + e_c i_c \quad (2.2.3)$$

$$q = e_\alpha \times i_\beta + e_\beta \times i_\alpha \quad (2.2.4)$$

where p and q are the real and imaginary power space vectors respectively. Rewrite the above equations in matrix form:

$$\begin{bmatrix} p \\ q \end{bmatrix} = \begin{bmatrix} e_\alpha & e_\beta \\ -e_\beta & e_\alpha \end{bmatrix} \begin{bmatrix} i_\alpha \\ i_\beta \end{bmatrix} \quad (2.2.5)$$

The inverse of (2.2.5) is:

$$\begin{bmatrix} i_\alpha \\ i_\beta \end{bmatrix} = \begin{bmatrix} e_\alpha & e_\beta \\ -e_\beta & e_\alpha \end{bmatrix}^{-1} \begin{bmatrix} p \\ q \end{bmatrix} \quad (2.2.6)$$

The instantaneous power on α - β coordinates are decomposed into two components, dc and ac:

$$p = p_{dc} + p_{ac} \quad (2.2.7)$$

$$q = q_{dc} + q_{ac}$$

The ac component represents the harmonics. Then the current in (2.2.6) can be separated into ac and dc parts:

$$\begin{aligned} \begin{bmatrix} i_{\alpha} \\ i_{\beta} \end{bmatrix} &= \begin{bmatrix} e_{\alpha} & e_{\beta} \\ -e_{\beta} & e_{\alpha} \end{bmatrix}^{-1} \begin{bmatrix} p_{dc} \\ q_{dc} \end{bmatrix} + \begin{bmatrix} e_{\alpha} & e_{\beta} \\ -e_{\beta} & e_{\alpha} \end{bmatrix}^{-1} \begin{bmatrix} p_{ac} \\ q_{ac} \end{bmatrix} \\ &= \begin{bmatrix} i_{\alpha_dc} \\ i_{\beta_dc} \end{bmatrix} + \begin{bmatrix} i_{\alpha_ac} \\ i_{\beta_ac} \end{bmatrix} = i_{dc} + i_{ac} \end{aligned} \quad (2.2.8)$$

where i_{α_dc} is α - axis instantaneous fundamental current
 i_{α_ac} is α - axis instantaneous harmonic current
 i_{β_dc} is β - axis instantaneous fundamental current
 i_{β_ac} is β - axis instantaneous harmonic current

Since the ac component in (2.2.8) represents the harmonics in the power line, the active filter can use this component to generate the compensating current. Therefore the compensating current in $\alpha\beta$ frame can be expressed as:

$$\begin{bmatrix} i_{\alpha_ac} \\ i_{\beta_ac} \end{bmatrix} = \begin{bmatrix} e_{\alpha} & e_{\beta} \\ -e_{\beta} & e_{\alpha} \end{bmatrix}^{-1} \begin{bmatrix} p_{ac} \\ q_{ac} \end{bmatrix} \quad (2.2.9)$$

First, a high-pass filter can be used to extract the ac power components: p_{ac} and q_{ac} . Second, the $\alpha\beta$ compensating currents can be obtained using (2.2.9). Third, the $\alpha\beta$ current can be transformed back to $a-b-c$ frame using the inverse transformation of (2.2.2), and the three-phase currents can be expressed as:

$$\begin{bmatrix} i_{ah} \\ i_{bh} \\ i_{ch} \end{bmatrix} = \sqrt{2/3} \begin{bmatrix} 1 & 0 \\ -1/2 & \sqrt{3}/2 \\ -1/2 & -\sqrt{3}/2 \end{bmatrix} \begin{bmatrix} i_{\alpha_ac} \\ i_{\beta_ac} \end{bmatrix} \quad (2.2.10)$$

Finally, the control reference of the three-phase compensating currents for active filter operation is given in (2.2.10).

2.2.2 Synchronous Detection

The synchronous detection method is based on the assumption that the three-phase supply current is balanced after compensation [6, 19]. The real power consumed by the load can be expressed as:

$$p = [e_a \quad e_b \quad e_c] \cdot \begin{bmatrix} i_{La} \\ i_{Lb} \\ i_{Lc} \end{bmatrix} \quad (2.2.11)$$

The real power p is sent to a low pass filter to obtain its average value P_{dc} . Using this value, the three-phase powers can be obtained as follows:

$$\begin{aligned} P_a &= \frac{P_{dc} E_a}{E_s} \\ P_b &= \frac{P_{dc} E_b}{E_s} \\ P_c &= \frac{P_{dc} E_c}{E_s} \end{aligned} \quad (2.2.12)$$

where E_a , E_b , and E_c are the amplitudes of the supply voltages, and $E_s = E_a + E_b + E_c$. The desired supply current can be expressed as follows:

$$\begin{aligned}
i_a &= \frac{2P_a e_a}{E_a^2} \\
i_b &= \frac{2P_b e_b}{E_b^2} \\
i_c &= \frac{2P_c e_c}{E_c^2}
\end{aligned}
\tag{2.2.13}$$

The compensating currents can be obtained by subtracting the currents of (2.2.13) from the original power line currents, $i_{L a,b,c}$.

$$\begin{aligned}
i_{ah} &= i_{La} - i_a \\
i_{bh} &= i_{Lb} - i_b \\
i_{ch} &= i_{Lc} - i_c
\end{aligned}
\tag{2.2.14}$$

Finally, the control reference for the active filter to generate the compensating current required to cancel the power line distortion is given in (2.2.14) [19].

2.3 Concept of Adaptive Noise Detection

The study above has identified areas of insufficiency in the detection of power line harmonics that can conclude the need of an effective detection method. This section presents the concept of an effective, adaptive harmonic detection method that is developed in this thesis research for the power line active filtering applications. The adaptive power line harmonic detection method developed in this thesis is based on the theory of adaptive noise cancellation. The theory was proposed originally for signal processing operation to cancel the noise combined in a signal or to separate the good signals from the noisy signals [11]. The theory can be illustrated using Figure 2.3.

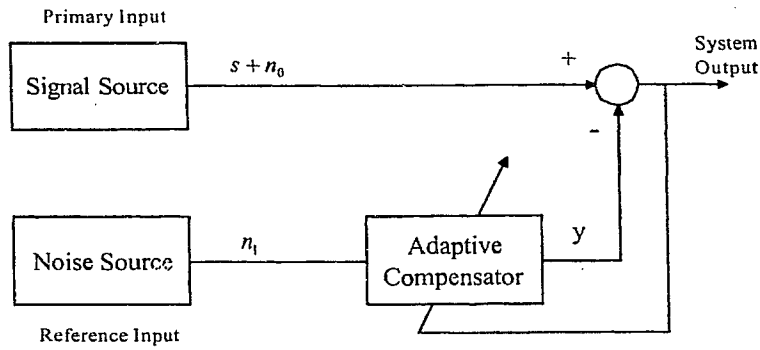


Figure 2.3: Block diagram for adaptive noise cancellation

A signal is transmitted over a channel to a sensor that receives the signal " s " plus an uncorrelated noise " n_0 ". The combined signal and noise " $s + n_0$ " form the primary input to the noise canceller. A second sensor receives a noise " n_1 " that is uncorrelated with the signal but correlated in some unknown way with the noise " n_0 ". This sensor provides the reference input to the noise canceller. The noise " n_1 " is used to produce a compensating signal " y " that is close replica of " n_0 ". Then this compensating signal is subtracted from the primary input " $s + n_0$ " to produce the system output " $s + n_0 - y$ ".

The adaptive noise canceller processes the reference input and automatically adjusts the impulse response through a least-squares algorithm such as the least-mean-square algorithm that responds to an error signal dependent on the canceller output. With the use of a proper algorithm, the canceller can operate under changing conditions and can adjust its output continuously to minimize the error signal.

The objective of the adaptive noise canceller is to produce a system output " $s + n_0 - y$ " that can best fit in the least-squares sense to the signal " s ". This objective can be accomplished by feeding the system output back to the noise canceller and adjusting the canceller through

an adaptive algorithm to minimize the total system output power. The system output serves as the error signal for the adaptive process.

Assume that s , n_0 , n_1 , and y are statistically stationary and have zero means. Also assume that s is uncorrelated with n_0 and n_1 , and n_1 is correlated with n_0 . Then the output becomes:

$$\varepsilon = s + n_0 - y \quad (2.3.1)$$

Squaring both side of (2.3.1), one obtains:

$$\varepsilon^2 = s^2 + (n_0 - y)^2 + 2s(n_0 - y) \quad (2.3.2)$$

Taking expectations of both sides of (2.3.2), and realizing that s is uncorrelated with n_0 and y , this yields:

$$\begin{aligned} E[\varepsilon^2] &= E[s^2] + E[(n_0 - y)^2] + 2E[s(n_0 - y)] \\ &= E[s^2] + E[(n_0 - y)^2] \end{aligned} \quad (2.3.3)$$

Accordingly, the minimum output power is

$$E_{\min}[\varepsilon^2] = E[s^2] + E_{\min}[(n_0 - y)^2] \quad (2.3.4)$$

When the canceller is adjusted so that $E[\varepsilon^2]$ is minimized, $E[(n_0 - y)^2]$ is therefore also minimized. The canceller output y is then the best least-squares estimate of the primary noise n_0 . Moreover when $E[(n_0 - y)^2]$ is minimized, $E[(\varepsilon - s)^2]$ is also minimized. From (2.3.1),

$$(\varepsilon - s) = (n_0 - y) \quad (2.3.5)$$

Adjusting or adapting the canceller to minimize the total output power is thus equivalent to causing the output ε to be the best least-squares estimate of the signal s for the given structure and adjustability of the adaptive compensator and for the given reference input.

From (2.3.3), the smallest possible output power is $E_{\min}[\varepsilon^2] = E[s^2]$. When this is achievable, $E[(n_0 - y)^2] = 0$. Therefore, $y = n_0$ and $\varepsilon = s$. In this case, minimizing output power causes the output signal to be perfectly free of noise.

Many algorithms can be used for the adaptive noise cancellation. In this thesis, the least-mean-squares algorithm has been used for elimination of harmonic distortions in the power line. The detailed formulation for adaptive harmonics filtering will be given in Chapter 3.

2.4 Concluding Remarks

The harmonic detection is an important component in the control of active filters. This chapter has presented the conventional harmonic detection methods, both in frequency domain and in time domain. The time domain method, in general, can provide a better detection than the frequency domain method. Areas of insufficiency for the conventional methods have been identified in this chapter.

The time domain methods, for example the instantaneous reactive power method and the synchronous detection method, work well only when the load is balanced and the supply voltage is un-distorted and balanced. The performance of the instantaneous reactive power method will degrade when the load is unbalanced and/or the supply voltage is distorted or unbalanced. The synchronous detection method gives poor results if the load is unbalanced or the supply voltage is distorted. Also both methods need a low-pass or high-pass filter to extract the power line harmonics. Their performance therefore is affected by the design of

the low-pass or high-pass filter, of which the output accuracy is largely subjected to the restrictions of bandwidth and to the sensitivity to frequency drift .

This chapter, based on the findings of the study on the conventional harmonic detection methods, has concluded that there is the need for an effective method for power line harmonic detections. This chapter has presented the theory of an adaptive detection method. This theory was proposed originally for signal processing operation to cancel the noise combined in a signal or to separate the good signals from the noisy signals. Based on this theory, an adaptive detection method for various power line distortion conditions is developed. Chapter 3 will provide the details of the development of the method.

Chapter 3

Adaptive Harmonic Detection Method For Active Filter Controls

This chapter presents the adaptive harmonic detection method developed in this thesis research for the control of active filters. The focus of this chapter is to detail the adaptive harmonic detection algorithm, and to apply this algorithm for active filter control. The adaptive harmonic detection algorithm is developed in this chapter, based on the theory of adaptive noise cancellation originally designed for signal processing. This thesis research applies this theory successfully in power engineering application, for the control of active power line filters.

The following lists the sections in this chapter.

Section 3.1 presents the adaptive harmonic detection method. In this section, the formulations for the detection are derived based on the theory of noise cancellation. The focus of this section is to provide simple expressions that can be easily used in active filters.

Section 3.2 discusses the application of the adaptive algorithm for power line harmonic detection.

Section 3.3 provides the theoretical requirements for the accuracy of the adaptive harmonic detection method. As the conditions of satisfying the requirements, this section

shows the mathematical uncorrelation between the line voltage and the compensating current, as well as the uncorrelation between the fundamental line current and the compensating current.

Section 3.4 presents the Simulink model for the adaptive noise-cancelling algorithm.

Section 3.5 provides the concluding remarks of this chapter.

3.1 Adaptive Harmonic Detection Algorithm

The adaptive harmonic detection method developed in this thesis uses the theory of adaptive noise cancellation to detect the harmonics in the power line. The basic concept has been presented in Section 2.3. This section presents the formulations for this adaptive noise cancellation algorithm. The formulations are particularly tailored in the form that can easily be used for the detection of power line harmonic distortion [11].

The structure of the adaptive noise cancellation algorithm can be illustrated using Figure 3.1. The algorithm can also be referred as an adaptive linear combiner.

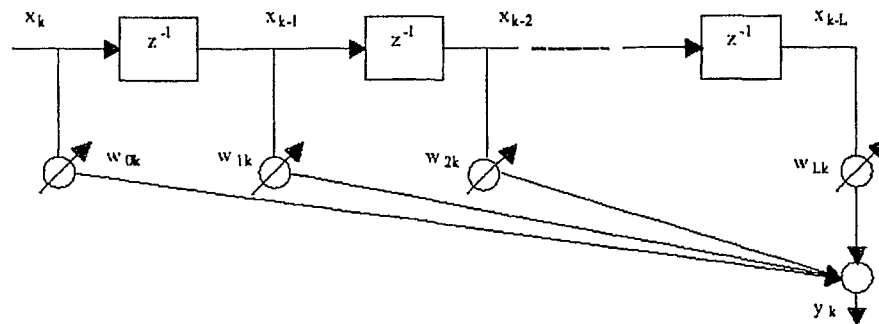


Figure 3.1: Adaptive linear combiner

Figure 3.1 shows the reference input signal vector with elements x_0, x_1, \dots, x_L , a corresponding vector of adjustable weights, w_0, w_1, \dots, w_L , a summing unit, and a single output signal, y .

For the application of power line harmonic detection designed in this thesis research, the input signal vector will contain the sampling data of the power line voltages. The values of the weights vector will be changed adaptively according to the magnitude of the fundamental component of the line current in such a way that the resulting output signal will be equal to the fundamental line current. Then the harmonic distortion of the power line can be detected by subtracting the output signal from the original distorted line signal.

Let \mathbf{X}_k be the reference input vector and \mathbf{W}_k be the weight vector. \mathbf{X}_k has $L+1$ elements taken from sequential samples for the same reference input. \mathbf{X}_k and \mathbf{W}_k can be written as:

$$\mathbf{X}_k = [x_k \quad x_{k-1} \quad \dots \quad x_{k-L}]^T \quad (3.1.1)$$

$$\mathbf{W}_k = [w_{0k} \quad w_{1k} \quad \dots \quad w_{Lk}]^T \quad (3.1.2)$$

Then the output y can be expressed as:

$$y_k = \sum_{l=0}^L w_{lk} x_{k-l} \quad (3.1.3)$$

The adaptive compensator adjusts its weights w according to the error signal, so that its output y becomes the optimal estimate of the distortion. Equation (3.1.3) can be rewritten as follows by using the vector notation:

$$y_k = \mathbf{X}_k^T \mathbf{W}_k = \mathbf{W}_k^T \mathbf{X}_k \quad (3.1.4)$$

The basic adaptive operation of the harmonic detection is by changing the vector \mathbf{W}_k as the time index k , changes.

If let d_k be the distorted signal, the difference between the combiner output and the distorted signal can be defined as:

$$\varepsilon_k = d_k - y_k \quad (3.1.5)$$

Substituting (3.1.4) into this expression yields:

$$\varepsilon_k = d_k - \mathbf{X}_k^T \mathbf{W} = d_k - \mathbf{W}^T \mathbf{X}_k \quad (3.1.6)$$

Squaring both sides of (3.1.6) to obtain the instantaneous square error:

$$\varepsilon_k^2 = d_k^2 + \mathbf{W}^T \mathbf{X}_k \mathbf{X}_k^T \mathbf{W} - 2d_k \mathbf{X}_k^T \mathbf{W} \quad (3.1.7)$$

Assume that ε_k, d_k and \mathbf{X}_k are statistically stationary, and take the expected value of (3.1.7) over the time index k . Then the expected value of ε_k^2 can be expressed as:

$$E[\varepsilon_k^2] = E[d_k^2] + \mathbf{W}^T E[\mathbf{X}_k \mathbf{X}_k^T] \mathbf{W} - 2E[d_k \mathbf{X}_k^T] \mathbf{W} \quad (3.1.8)$$

Note that the expected value of any sum is the sum of expected values, but that the expected value of a product is the product of expected values when the variables are statistically independent. The signals x_k and d_k are not generally independent.

The mean-square-error function can be conveniently expressed as follows. Let \mathbf{R} be defined as the square matrix:

$$\mathbf{R} = E[\mathbf{X}_k \mathbf{X}_k^T] = E \begin{bmatrix} x_k^2 & x_k x_{k-1} & x_k x_{k-2} & \dots & x_k x_{k-L} \\ x_k x_{k-1} & x_{k-1}^2 & x_{k-1} x_{k-2} & \dots & x_{k-1} x_{k-L} \\ \dots & \dots & \dots & \dots & \dots \\ x_k x_{k-L} & x_{k-1} x_{k-L} & x_{k-2} x_{k-L} & \dots & x_{k-L}^2 \end{bmatrix} \quad (3.1.9)$$

This matrix is designated the "input correlation matrix". The main diagonal terms are the mean squares of the input components, and the cross terms are the cross correlations among the input components. Let \mathbf{P} be similarly defined as a column vector:

$$\mathbf{P} = E[d_k \mathbf{X}_k] = E[d_k x_k \quad d_k x_{k-1} \quad \dots \quad d_k x_{k-L}]^T \quad (3.1.10)$$

Let the mean-square error in (3.1.8) be designated by ξ and express it in terms of (3.1.9) and (3.1.10) as:

$$\text{MSE} \equiv \xi = E[\varepsilon_k^2] = E[d_k^2] + \mathbf{W}^T \mathbf{R} \mathbf{W} - 2 \mathbf{P}^T \mathbf{W} \quad (3.1.11)$$

The objective of adaptive operation is to find the value of \mathbf{W} such that the mean-square error ξ is minimum. The gradient of the mean-square-error function (3.1.11), designated as $\nabla(\xi)$ or simply ∇ , can be obtained by differentiating (3.1.11) to obtain the column vector:

$$\begin{aligned} \nabla &= \frac{\partial \xi}{\partial \mathbf{W}} = \left[\frac{\partial \xi}{\partial w_0} \quad \frac{\partial \xi}{\partial w_1} \quad \dots \quad \frac{\partial \xi}{\partial w_L} \right] \\ &= 2 \mathbf{R} \mathbf{W} - 2 \mathbf{P} \end{aligned} \quad (3.1.12)$$

where \mathbf{R} and \mathbf{P} are given by (3.1.9) and (3.1.10) respectively.

The mean-square error is minimized if the weight vector can be set at its optimal value \mathbf{W}^* where the gradient is zero. This condition can be expressed as:

$$\nabla = \mathbf{0} = 2 \mathbf{R} \mathbf{W}^* - 2 \mathbf{P} \quad (3.1.13)$$

Several methods can be used to search the optimal value W^* . One method is called steepest descent gradient search method. In this method, the weight vector W is updated at each step according to the following equation:

$$W_{k+1} = W_k + \mu(-\nabla_k) \quad (3.1.14)$$

where μ is a constant that regulates the step size and is chosen such that:

$$0 < \mu < \frac{1}{\lambda_{\max}} \quad (3.1.15)$$

where λ_{\max} is the largest eigenvalue of R . The steepest method is general stable and convergent.

Recall the adaptive linear combiner as shown in Figure 3.2.

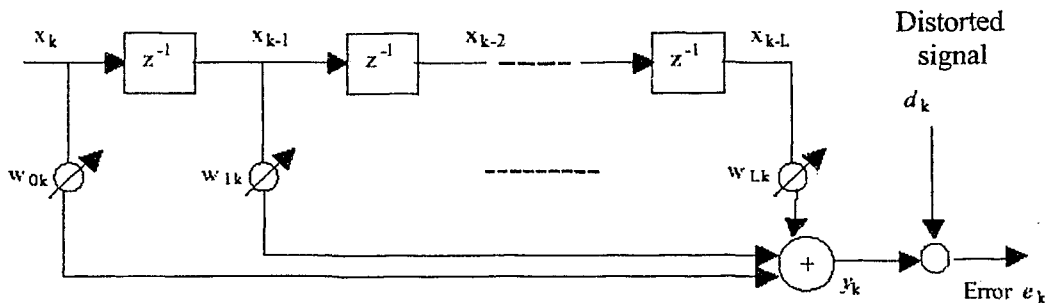


Figure 3.2: The adaptive compensator

From (3.1.6), the error signal ϵ_k between the combiner output and the distorted signal is:

$$\epsilon_k = d_k - X_k^T W_k \quad (3.1.16)$$

To develop the adaptive algorithm from (3.1.14), one needs to estimate the gradient of $\xi = E[\epsilon_k^2]$ at each sampling period and update the weight vector W . The estimation can be

done by taking differences between short-term averages of ε_k^2 . However, in the least-mean-squares algorithm, ε_k^2 is taken as an estimate of ξ_k :

$$\begin{aligned}\varepsilon_k^2 &= (d_k - \mathbf{X}_k^T \mathbf{W}_k)^2 = (d_k - \mathbf{W}_k^T \mathbf{X}_k)^2 \\ &= d_k^2 - 2d_k \mathbf{W}_k^T \mathbf{X}_k + (\mathbf{W}_k^T \mathbf{X}_k)^2\end{aligned}\quad (3.1.17)$$

The estimated gradient can be written as:

$$\begin{aligned}\hat{\nabla}_k &= \frac{\partial \varepsilon_k^2}{\partial \mathbf{W}_k} = 0 - 2d_k \mathbf{X}_k + 2(\mathbf{W}_k^T \mathbf{X}_k) \mathbf{X}_k \\ &= -2(d_k - \mathbf{W}_k^T \mathbf{X}_k) \mathbf{X}_k \\ &= -2\varepsilon_k \mathbf{X}_k\end{aligned}\quad (3.1.18)$$

Then, at each iteration in the adaptive process, the gradient estimate has the form of:

$$\hat{\nabla}_k = \begin{bmatrix} \frac{\partial \varepsilon_k^2}{\partial w_0} \\ \vdots \\ \frac{\partial \varepsilon_k^2}{\partial w_0} \end{bmatrix} = 2\varepsilon_k \begin{bmatrix} \frac{\partial \varepsilon_k}{\partial w_0} \\ \vdots \\ \frac{\partial \varepsilon_k}{\partial w_0} \end{bmatrix} = -2\varepsilon_k \mathbf{X}_k\quad (3.1.19)$$

With this simple estimate of the gradient, a steepest-descent type of adaptive algorithm is formed. From (3.1.14), one obtains:

$$\begin{aligned}\mathbf{W}_{k+1} &= \mathbf{W}_k - \mu \hat{\nabla}_k \\ &= \mathbf{W}_k + 2\mu \varepsilon_k \mathbf{X}_k\end{aligned}\quad (3.1.20)$$

This is the least-mean-squares adaptive algorithm. μ is the performance factor which regulates the speed and stability of adaptation. The adaptive noise cancellation algorithm shown in Figure 3.2 can now be summarized as follows:

The output of the adaptive compensator y_k can be expressed as:

$$y_k = \sum_{l=0}^L w_{lk} x_{k-l} \quad (3.1.21)$$

The output of the system is served as an error signal as well. Then the error signal is used to adjust the weights of the adaptive compensator, as indicated in (3.1.22). Therefore the error is minimized.

$$w_{l(k+1)} = w_{lk} + 2\mu e_k x_{k-l} \quad l = 0, 1 \dots L \quad (3.1.22)$$

3.2 Application of Adaptive Noise Cancellation Algorithm For Harmonic Detection

In power line harmonic detection, it is difficult to directly determine the amplitude and phase of each harmonic component in power line current prior to carrying out the analysis of the harmonic contents. On the other hand, if the fundamental component of the power line current can be obtained, the total harmonic distortion then can be calculated simply by subtracting the fundamental component from the measured power line current. Therefore the major task of the harmonic detection using the adaptive noise cancellation algorithm is to extract the fundamental component from harmonic-polluted power line current.

Let $i_L(t)$ be the power line current that has been contaminated by harmonics generated by the non-linear loads. $i_L(t)$ can be decomposed into a series of sinusoidal component by Fourier transformation:

$$\begin{aligned} i_L(t) &= I_1 \sin(\omega t + \varphi_1) + \sum_{n=2}^{\infty} I_n \sin(n\omega t + \varphi_n) \\ &= i_1(t) + i_h(t) \end{aligned} \quad (3.2.1)$$

where i_l is the fundamental component, and i_h is the sum of harmonics. $i_l(t)$ can be decomposed into an active part and a reactive part. Equation (3.2.1) can be rewritten as:

$$i_L(t) = I_1 \sin(\omega t + \varphi_1) + \sum_{n=2}^{\infty} I_n \sin(n\omega t + \varphi_n) \quad (3.2.2)$$

$$= i_a(t) + i_{comp}(t)$$

where i_a represents the in-phase line current, and i_{comp} represents the harmonic current component needed to be compensated.

Figure 3.3 shows the block diagram for the active filter control using the adaptive noise cancellation algorithm for power line harmonic detection.

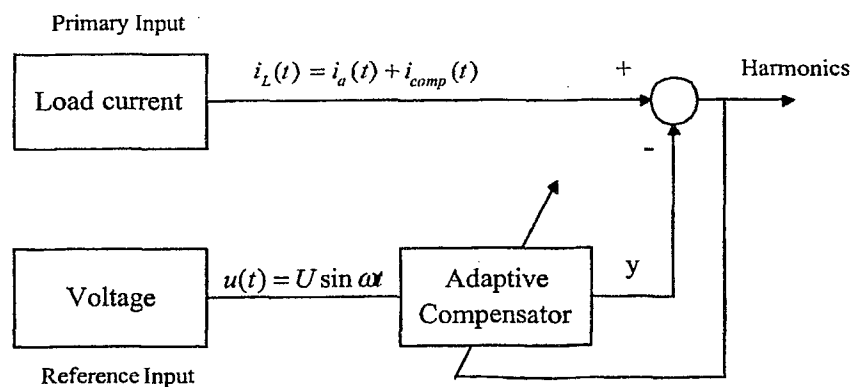


Figure 3.3: Application of adaptive noise cancellation for power line harmonic detection

The primary input is the power line current. For the reference input, we can use the source voltage. The adaptive compensator will adjust its weights constantly so that its output y is the best estimate of the fundamental component. By subtracting the estimated fundamental part y , the harmonics are determined.

Recall the algorithm of adaptive noise cancellation, as illustrated in Figure 2.3. The pre-conditions for the method to function, i.e. to cancel the noise in a signal, are:

- The signal s and the noise n_0 are uncorrelated.
- The reference input n_1 is uncorrelated to the signal s , but n_1 is correlated to the noise n_0 .

Obviously, in Figure 3.3, the utility voltage u and the line current i_a are correlated. In order to apply the algorithm of the adaptive noise cancellation successfully, it is necessary to show the following two conditions:

- The line current i_a and the compensating current i_{comp} are uncorrelated.
- The utility voltage u and the compensating current i_{comp} are uncorrelated.

3.3 Uncorrelation between u and i_{comp} and between i_a and i_{comp}

The following shows that u and i_{comp} are uncorrelated and similarly i_a and i_{comp} are also uncorrelated.

In this thesis, u is the power line voltage and can be expressed as:

$$u(t) = U \sin \omega t \quad (3.3.1)$$

i_{comp} is the compensated current for the elimination of power line current harmonics and can be written as:

$$i_{comp} = i_q + i_{c2} + i_{c3} + \dots + i_{cn} = i_q + \sum_{n=2}^{\infty} I_n \sin(n\omega t + \varphi_n) \quad (3.3.2)$$

where i_q is the reactive part of the power line current, i_{cn} is the n^{th} harmonic current.

u and i_{comp} are definite in $[-T/2, T/2]$, where T is the period of 60 Hz. Assume that there exists a set of constant, $c_0, c_1, c_2, \dots, c_n, \dots$, such that

$$\begin{aligned} c_0 u + c_1 i_q + c_2 i_{c2} + c_3 i_{c3} + \dots + c_n i_{cn} &= 0 \\ c_0 U \sin \omega + c_1 i_q + \sum_{n=2}^{\infty} c_n I_n \sin(n\omega + \varphi_n) &= 0 \end{aligned} \quad (3.3.3)$$

Multiply (3.3.3) with $\sin \omega$ and perform integration on both sides from $-T/2$ to $T/2$, then one can obtain

$$\begin{aligned} &\int_{-T/2}^{T/2} c_0 U (\sin \omega)^2 dt + \int_{-T/2}^{T/2} c_1 i_q U \sin \omega dt + \sum_{n=2}^{\infty} \int_{-T/2}^{T/2} c_n I_n \sin(n\omega + \varphi_n) \sin \omega dt \\ &= c_1 U \int_{-T/2}^{T/2} (\sin \omega)^2 dt + \int_{-T/2}^{T/2} c_1 i_q U \sin \omega dt + \sum_{n=2}^{\infty} c_n I_n \int_{-T/2}^{T/2} \sin(n\omega + \varphi_n) \sin \omega dt \\ &= 0 \end{aligned} \quad (3.3.4)$$

From the orthogonal property of sine functions, the second term and third term of (3.3.4) are always zero. Therefore, the first term of (3.3.4) must be zero, that is

$$c_1 U \int_{-T/2}^{T/2} (\sin \omega)^2 dt = 0 \quad \text{for all } t \in [-T/2, T/2] \quad (3.3.5)$$

Because $U \int_{-T/2}^{T/2} (\sin \omega)^2 dt \neq 0$ ($t \neq 0$), equation (3.3.5) is true for all $t \in [-T/2, T/2]$ if and only if

$$c_1 = 0 \quad (3.3.6)$$

Similarly, multiply (3.3.3) with $\sin(n\omega)$ where $n = 2, 3, \dots, \infty$ and perform integration on both sides, then one can obtain

$$c_n = 0 \quad \text{for } n = 2, 3, \dots, \infty \quad (3.3.7)$$

The above two equations show that all the coefficients of (3.3.3) are zeros. Therefore, by mathematical definitions, u and i_{comp} are independent and they are uncorrelated also.

With a similar approach as the above, it can be shown that i_a and i_{comp} are uncorrelated.

3.4 Simulink Model For Adaptive Noise Cancelling Algorithm

The adaptive noise-cancelling algorithm can be simulated using the program Simulink in the computer software MATLAB. Figure 3.4 shows the Simulink model for the adaptive noise-cancelling algorithm.

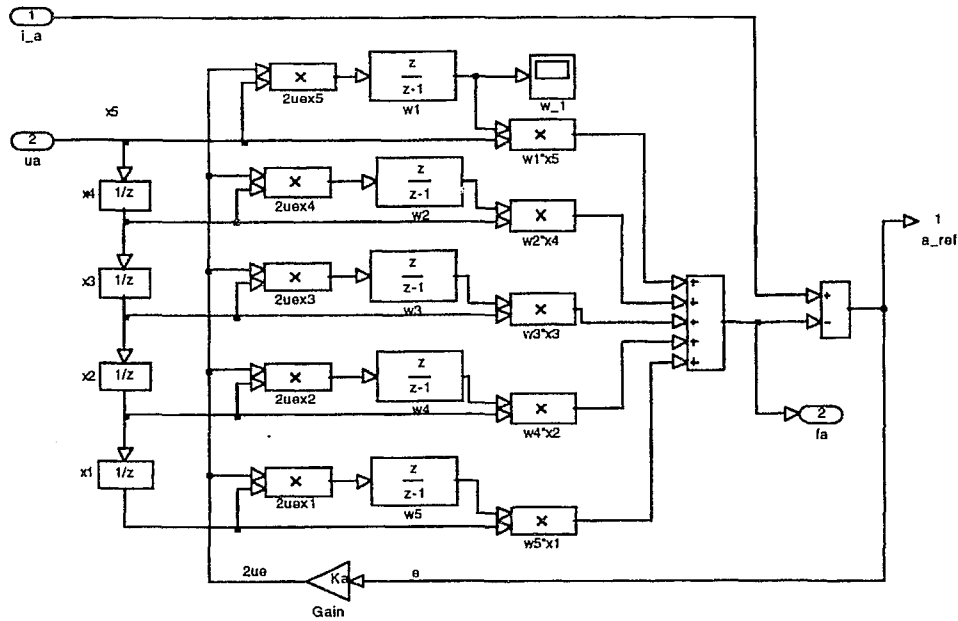


Figure 3.4: Model of adaptive noise cancelling algorithm

In this figure,

Input1: the load current which is the primary input of the adaptive algorithm.

Input2: source voltage which is the reference input of the algorithm.

output1: the detected harmonic current.

output2: the adaptive compensator output which is the estimated fundamental component.

w_1, w_2, \dots, w_5 are the weights of the adaptive compensator.

e : the error signal.

μ performance factor that regulates the convergence speed and stability of the algorithm.

The performance factor μ has a range of $0 < \mu < 1$.

3.5 Concluding Remarks

This chapter has presented an adaptive harmonic detection method for the application of active power line filtering. In this chapter, the formulations for the noise cancellation operation have been derived in such expressions that can be easily applied for power line harmonic detections.

In the adaptive algorithm presented in this chapter, each component of the gradient vector is obtained from a single data sample without perturbing the weight vector, and the least-mean-square algorithm updates the weights at each step according to the error signal. This algorithm can be easily implemented in a practical digital processor without squaring, averaging, or differentiation and is elegant in its simplicity and efficiency.

Chapter 4

Effectiveness of Adaptive Harmonic Detection Method For Control of Active Filter

This chapter provides the computer simulation results for demonstrating the effectiveness of the adaptive harmonic detection method developed in this thesis research. The verifications are carried out under different load and supply conditions. The results using the adaptive harmonic detection method are compared with those of two typical methods: the instantaneous reactive power method and the synchronous detection method. The capability of the method for adaptation to load changes is demonstrated in this chapter.

This chapter is organized as follows:

Section 4.1 presents the verification of the effectiveness of the adaptive detection using a square wave representing the power line current. This is a vigorous verification where the harmonic distortion of a square wave is known, and therefore the effectiveness of the detection method can be shown easily with a known reference. This section will verify the method for 4 conditions: current in phase with line voltage, current with a phase shift with the line voltage, current with changing amplitude, and different detection performance factors.

Section 4.2 shows the circuit configurations used for verification of the effectiveness of the adaptive harmonic detection method. These configurations represent typical non-linear loads found in the industry.

Section 4.3 presents the verification of the adaptive detection method for steady state operations under typical power line conditions. This section will show the effectiveness of the method for detection of power line distortion caused by rectifier carrying RL load or RLC load in combination with balanced or unbalanced line voltage or with unequal single-phase loads on the three-phase supply system.

Section 4.4 presents the verification of the adaptive detection method for a dynamic operation where two additional rectifier loads are switched in. This section will show the adaptive capability of the detection method developed in this thesis research.

Section 4.5 compares the adaptive detection method with two well-known conventional detection methods: the instantaneous reactive power method and the synchronous detection method. This section will show that the adaptive detection method performs better than the conventional methods particularly when the power line operates under abnormal conditions.

Section 4.6 provides concluding remarks of this chapter.

4.1 Verification Using a Square Wave With Known Harmonic Distortion

This section demonstrates the accuracy of the adaptive harmonic detection method using a square wave. The reason of using a square wave as a test signal is that the harmonics of a square wave are known, and therefore the detection results can be verified easily and accurately.

Four conditions are tested in this section:

1. Square wave in phase with a reference signal.
2. Square wave with a phase shift to the reference signal.
3. Square wave with changing amplitude.
4. Performances study for typical performance factors μ .

The reference signal is a sine wave that has the same frequency (60Hz) as the square wave.

4.1.1 Square Wave in Phase With Reference Signal

For convenient verification of the detection method, it is assumed that the measured signal of the load current is a square wave with the frequency of 60 Hz and the amplitude of 1 unit. A 60Hz sine wave in phase with the square wave is used as the reference signal. The detection results are shown in Figure 4.1, where (a) is the estimated fundamental component, and (b) is the detected harmonics of the square wave. This figure shows that the estimated waveforms match the ideal ones, and therefore the adaptive harmonic detection method has detected the harmonics accurately.

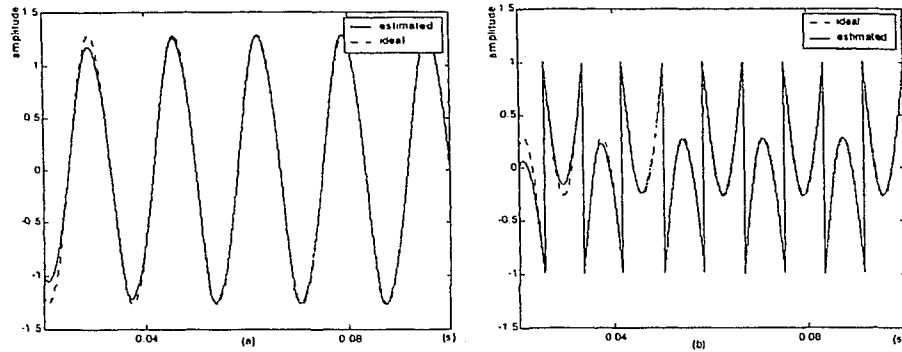


Figure 4.1: Verification of harmonic detection using a square wave
 (a) fundamental component, (b) total harmonics

4.1.2 Square Wave and Reference Signal Not in Phase

Another verification of the adaptive detection method deals with a simulation of the practical condition that the power line voltage and current are not in phase. This condition often exists in the industrial system that carries reactive and resistive loads. Figure 4.2 shows the results of verification when the reference sine wave has a phase shift of 36° , which is arbitrarily chosen with respect to the fundamental component of the square wave. For convenient verification, it is assumed that the square wave of 1 unit represents the load current and the sine wave represents the power line voltage. The figure shows a good match of the estimated waveform and the ideal waveform.

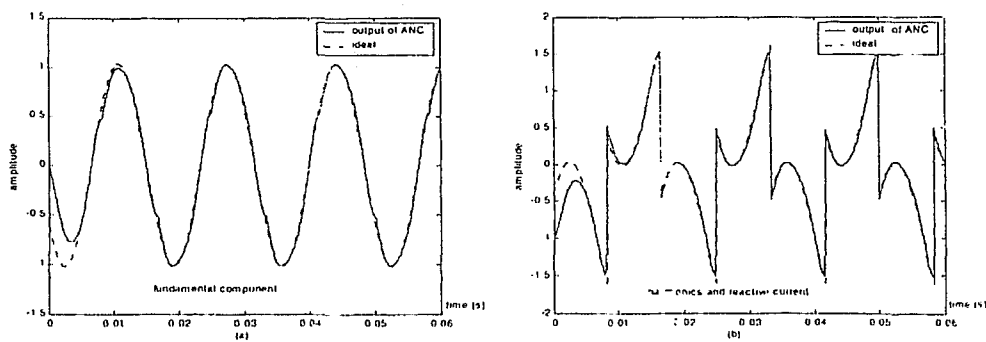


Figure 4.2: (a) In-phase fundamental component,
 (b) Total harmonic plus out-of-phase fundamental component

4.1.3 Square Wave With Changing Amplitude

In order to verify that the detection method can adapt to the changes of non-linear loads, a square wave with changing amplitude is used to represent the load current. The results of harmonic detection and the ideal waveforms are given in Figure 4.3. This figure shows that the detection method can adapt to the load changes very well.

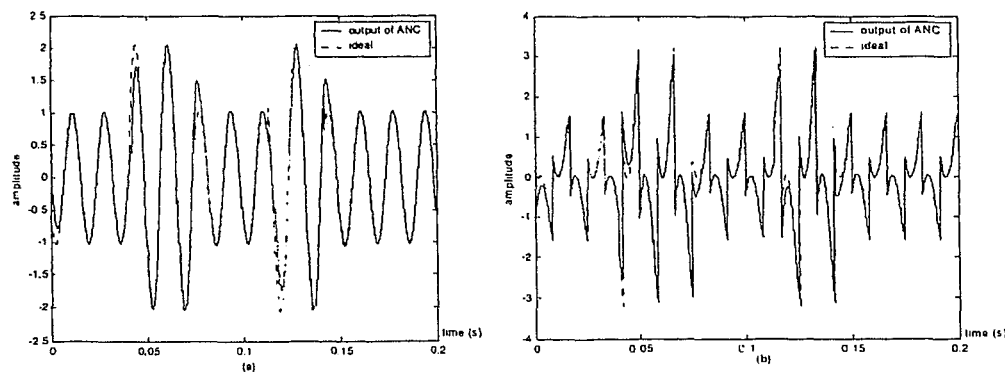


Figure 4.3: Harmonic detection of a square wave with changing amplitude
(a) Fundamental component, (b) Total harmonic component

4.1.4 Performances Study With Different Values of Performance Factor μ

As given in Section 3.1, μ is the performance factor that regulates the convergence of the adaptive harmonic detection method. If μ is too small, the system will take long time for its output to reach the desired value. On the other hand, if the performance factor is too large, the system will response fast but give large error. Two cases, one with a small performance factor $\mu = 2 \times 10^{-5}$ and the other with a large one $\mu = 10^{-4}$, have been tested. The results are shown in Figure 4.4 and Figure 4.5 respectively. Figure 4.4 shows that the system with a small μ takes 3 cycles to reach the ideal curve, and after it reaches the desired waveform, the

error is very small. However, as shown in Figure 4.5, the system with larger μ has a faster response time, but the error is relatively larger.

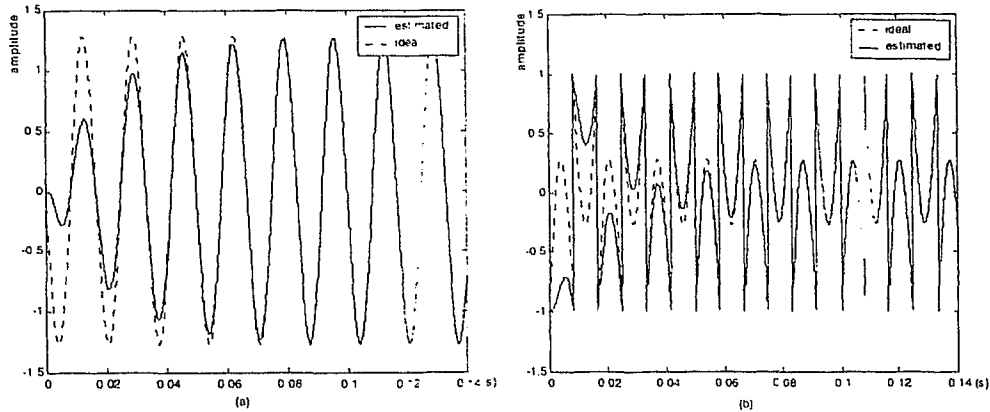


Figure 4.4: Output of the adaptive filter with $\mu = 2 \times 10^{-5}$
 (a) Fundamental component, (b) Total harmonics

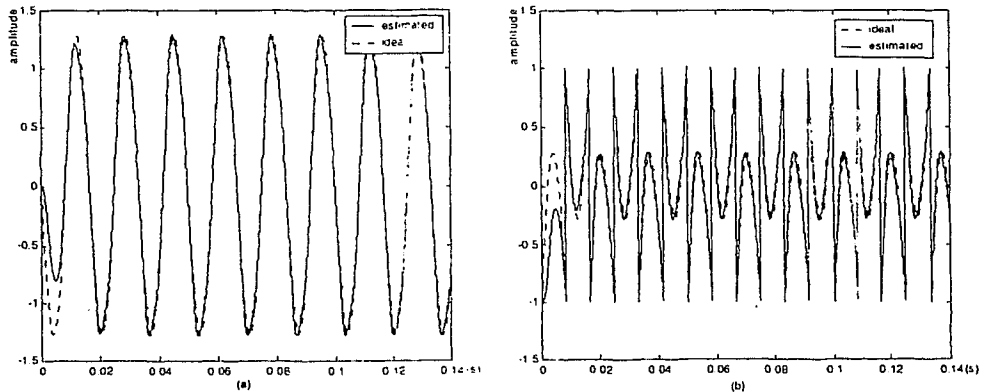


Figure 4.5: Output of the adaptive filter with $\mu = 10^{-4}$
 (a) Fundamental component, (b) Total harmonics

4.2 Modeling of Power Electronic Loads For Active Filtering Study

The above verification with a square wave has shown that the adaptive harmonic detection method can provide accurate detection results. In industry, there are different types of

nonlinear loads such as power electronic equipment that could generate higher amount of harmonics than a square-wave source dose. It is useful to verify the effectiveness of the adaptive harmonic detection method using typical power electronic loads with higher harmonic contents. For convenient verification, the following simulation models for typical power electronic loads have been built:

1. Rectifier with RL load as harmonic source on power line.
2. Rectifier with RLC load with higher harmonic injection on power line.
3. Unbalanced nonlinear load as a combination of rectifier and single-phase loads.

4.2.1 Rectifier With RL Load as Harmonic Source on Power Line

The first non-linear load model built for verification of the adaptive harmonic detection method developed in this thesis research is a power electronic rectifier with RL (resistive-inductive) load. Figure 4.6 shows the connection of an active filter for elimination of harmonics injected from the rectifier load. An example of this type of loads is the induction heating system used for forging, soldering, cooking, etc. This system can be simplified as a RL (resistive-inductive) load fed by a power electronic rectifier. As the rectifier converts ac power to dc power, it could generate substantial amount of harmonics at its input line [33, 34].

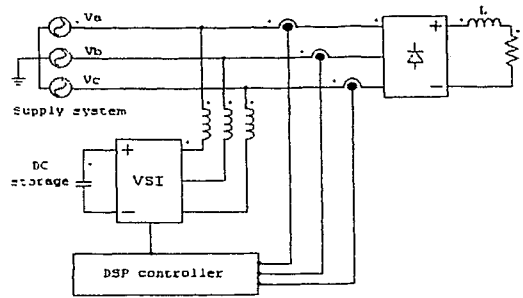


Figure 4.6: Active filtering of harmonics generated by rectifier with RL load

4.2.2 Rectifier With RLC Load With Higher Harmonic Injection on Power Line

The second non-linear load model built to verify the adaptive detection method is a rectifier with RLC (resistive-inductive-capacitive) load. With the capacitor C in the load, the rectifier will generate higher harmonics on the power line than that with the RL load. Active filter can be used to effectively suppress harmonics from this type of non-linear load. Figure 4.7 shows the connection of the active filter and the rectifier load.

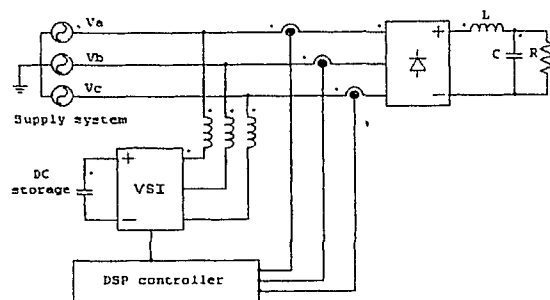


Figure 4.7: Active filtering of harmonics generated by rectifier with RLC load

4.2.3 Unbalanced Load as a Combination of Rectifier and Single-phase Loads

The third non-linear model built in this thesis research for verification of the detection method is a rectifier with a parallel-connected unbalanced load. This simulates the real

power system conditions where single-phase loads connected on each of the three phases in the system are not necessary equal. Figure 4.8 shows the connection of an active filter for suppression of harmonics under the unbalanced loading conditions.

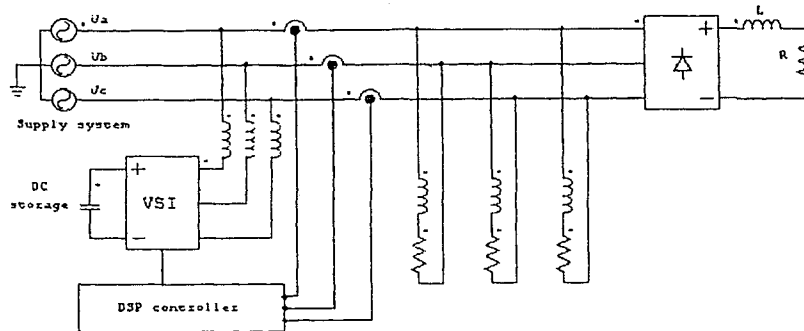


Figure 4.8: Active filtering of harmonics generated by unbalanced nonlinear loads

4.3 Verification of Adaptive Harmonic Detection Method for Steady State Operations

This section demonstrates the effectiveness of the adaptive harmonic detection method developed in this thesis research. The demonstration is carried out for typical power line conditions that are simulated as follows:

1. Harmonics from rectifier RL load with normal or unbalanced line voltage
2. Harmonics from rectifier RLC load with unbalanced line voltage
3. Harmonics from rectifier load with unbalanced single-phase loads

4.3.1 Harmonics From Rectifier RL Load With Normal or Unbalanced Line Voltage

In this section, the effectiveness of the adaptive detection method is tested for two simulated power line conditions: harmonics injected from a rectifier RL load under normal power line voltage, and harmonics under unbalanced line voltage. Figure 4.6 shows the circuit for the test.

1. Normal power line voltage

Figure 4.9 shows the simulation results for the detection of power line harmonic distortion caused by the rectifier with RL load with the normal balanced line voltage.

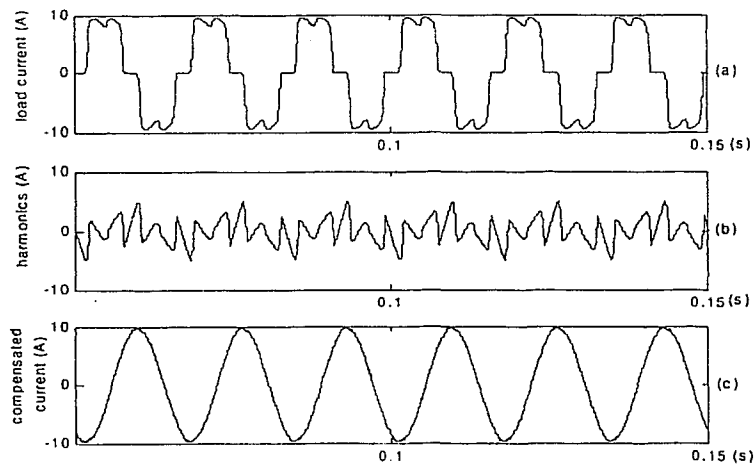


Figure 4.9: Detection for rectifier RL load under normal line voltage

In Figure 4.9, only the simulation results of Phase "a" are presented because the load is balanced and the results for all three phases are similar. The power line current prior to compensation has a 26.07% total harmonic distortion (THD). The THD of the power line

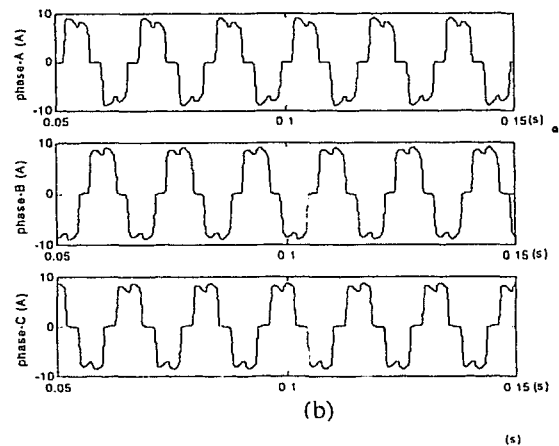
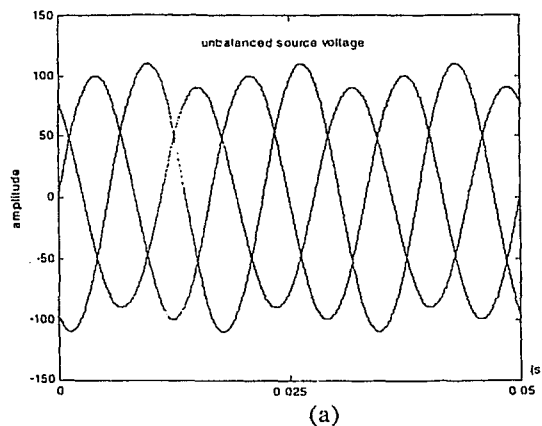
current after compensation is reduced to 1.05%. Table 4.1 lists the THD values of the power line current before and after compensation.

THD	Phase-A	Phase-B	Phase-C
Before compensation	26.07	26.07	26.07
After compensation	1.05	1.04	1.05

Table 4.1: THD (%) for the waveforms in Figure 4.9

2. *Unbalanced power line voltage*

The above shows that the adaptive harmonic detection method has provided accurate detection result when the load is balanced under the normal power line voltage. However, the power line voltage may not be always balanced. This section demonstrates the effectiveness of the adaptive method for detecting the power line distortion under a fairly severe unbalanced line voltage as shown in Figure 4.10(a).



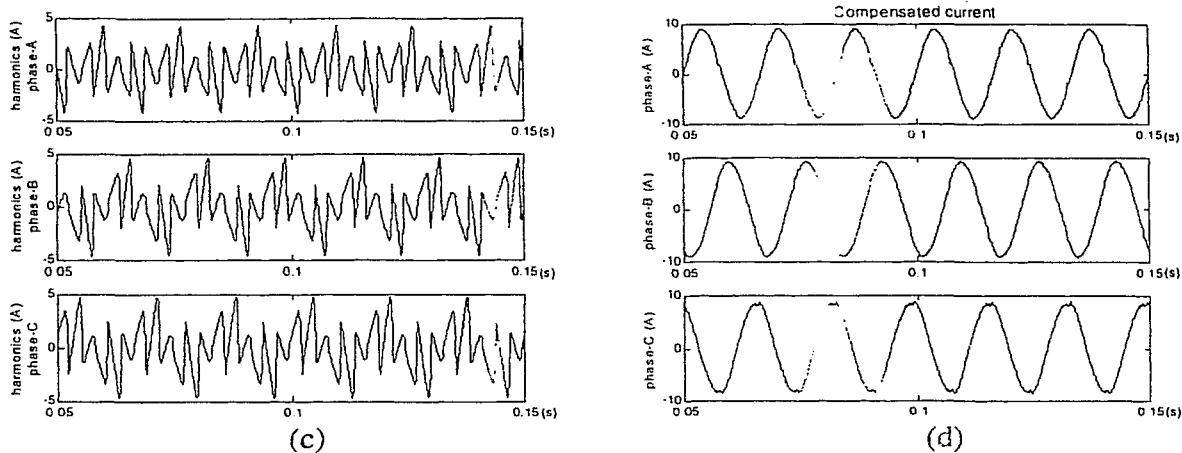


Figure 4.10: Detection for rectifier RL load under unbalanced line voltage

Figure 4.10 shows the rectifier load current in (b), the compensating harmonic distortion in (c), and the compensated power line current in (c). The THD before compensation has an average of 26.4%. After compensation, the THD is reduced to only 2.7%. Table 4.2 shows the values of the THD on each phase.

THD	Phase-A	Phase-B	Phase-C
Before compensation	26.96	25.01	27.20
After compensation	2.64	2.39	3.16

Table 4.2: THD (%) for the waveforms in Figure 4.10

4.3.2 Harmonics From Rectifier RLC Load With Unbalanced Line Voltage

In this section, the adaptive harmonic detection method is tested for a severe power line condition with a high harmonic distortion and with unbalanced line voltage. To simulate this condition, a rectifier with RLC load is used and the circuit is shown in Figure 4.7. The detection results are given in Figure 4.11.

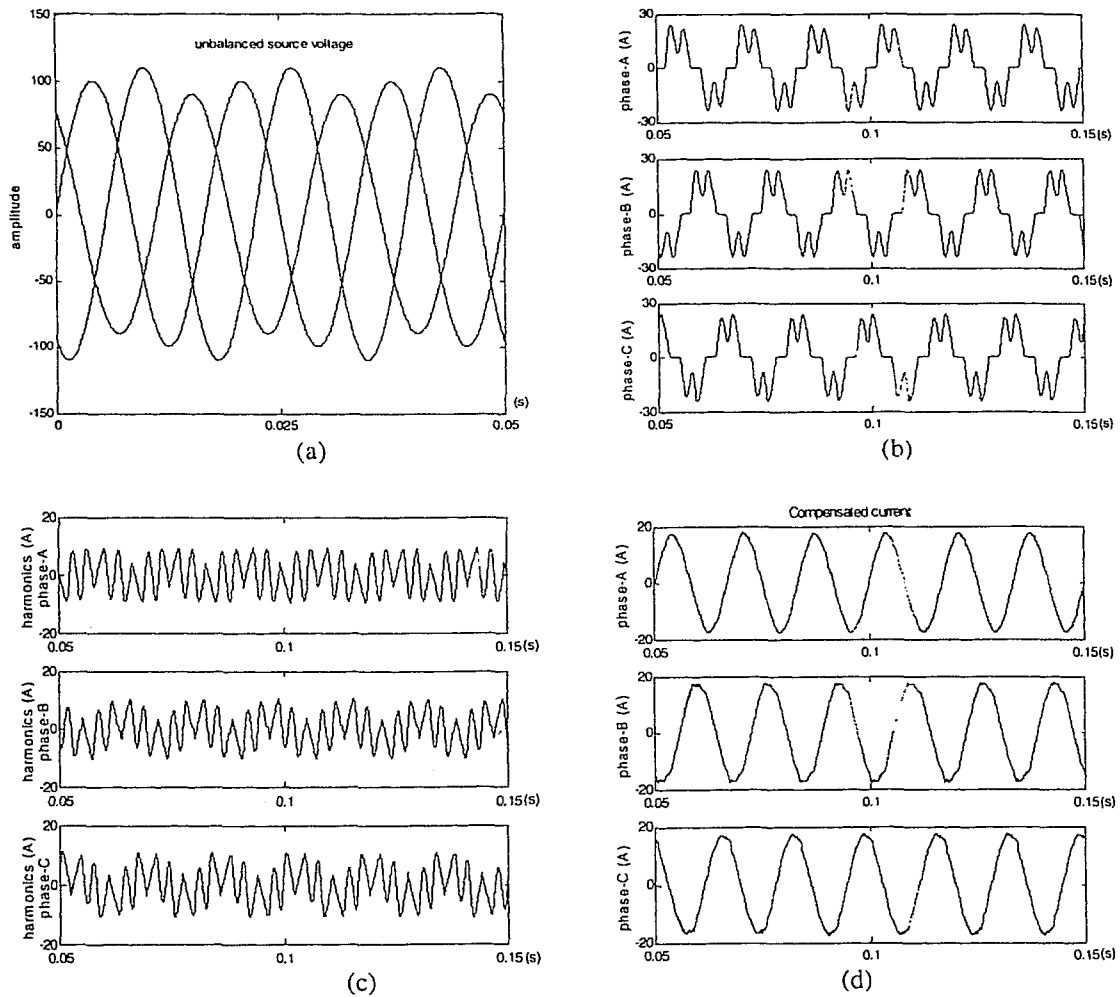


Figure 4.11: Detection for rectifier RLC load with non-ideal line voltage

Figure 4.11 shows the unbalanced line voltages in (a), the uncompensated line current in (b), the current harmonic distortion in (c), and the compensated power line current in (d). Table 4.3 shows the values of the line current THD before and after compensation on each phase. The power line current has an average THD of 42.9% before compensation. The power line current THD is reduced to an average of 3.2% after compensation.

THD	Phase-A	Phase-B	Phase-C
Before compensation	44.58	41.88	42.20
After compensation	2.76	3.91	2.86

Table 4.3: THD (%) for the waveforms in Figure 4.11

4.3.3 Harmonics From Rectifier Load With Unbalanced Single-phase Loads

Unbalanced power line current occurs when single-phase loads connected to a three-phase system are not equal on all phases, or when a three-phase load has unbalanced impedances. There may be some other nonlinear loads connected to the same supply system. Harmonics generated by the non-linear loads together with unbalanced currents from single-phase loads may circulate in the supply system and cause overheating problems. Active filter can be used to suppress harmonics and, in some cases, to correct the unbalanced conditions.

In this section, the effectiveness of the adaptive harmonic detection method is tested for a special power line condition where unbalanced line current is caused by three unequal single-phase RL loads and a rectifier load. Figure 4.8 shows the circuit used for this test. Figure 4.12 shows the simulation results.

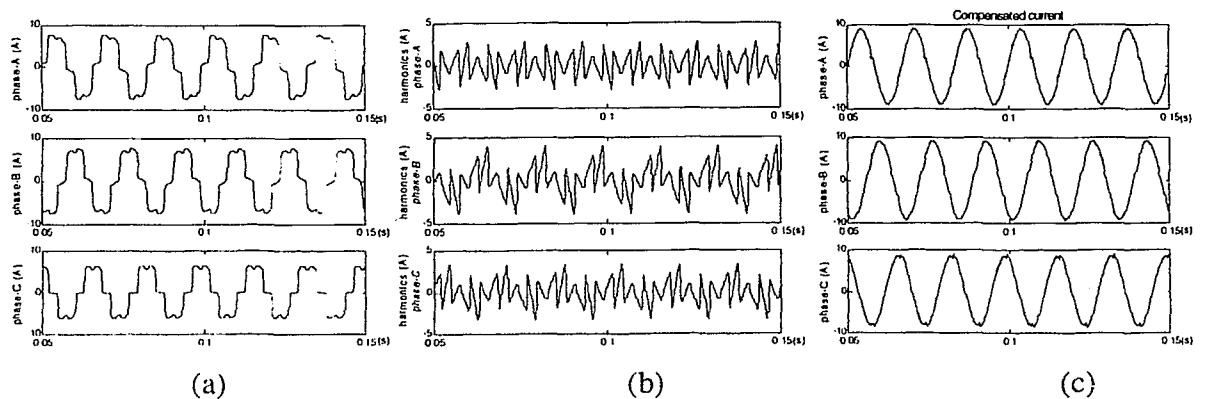


Figure 4.12: Detection for three unequal single-phase loads and a rectifier load.

Figure 4.12 shows the load currents in (a), the current harmonic distortions in (b), and the compensated power line currents in (c). Table 4.4 lists the values of current THD on the power line before and after harmonic compensation. The power line current before compensation has an average THD of 22.8%. The current THD is reduced to an average of 4.5% after compensation.

THD	Phase-A	Phase-B	Phase-C
Before compensation	22.61	22.93	22.84
After compensation	3.98	4.79	4.64

Table 4.4: THD (%) for waveforms in Figure 4.12

4.4 Verification of Adaptive Harmonic Detection Method For Dynamic Operation

This section demonstrates the adaptive capability of the detection method to the changes of power line condition. To simulate a dynamic condition, it is assumed that a rectifier load is connected on the power line, and after the first load reaches steady state, two rectifier loads (each of 40% of the first load) are connected with a time difference of approximately 4 cycles. This severe power line dynamic condition is used to test the accuracy and adaptive capability of the detection method developed in this thesis.

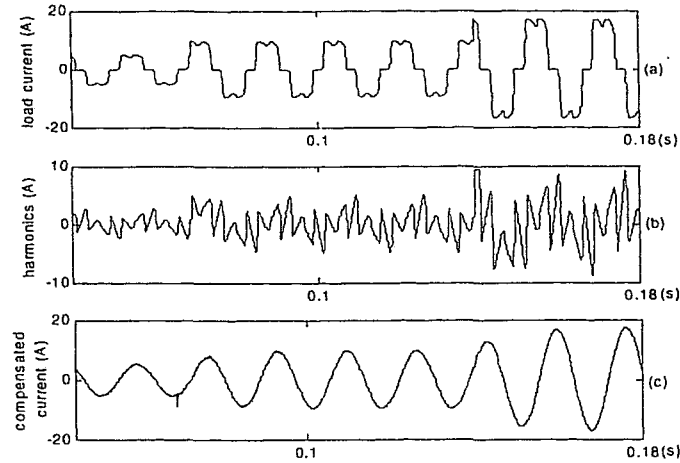


Figure 4.13: load current with changing amplitude

Figure 4.13 shows the detection results for the simulated severe dynamic power line condition. This figure shows (a) the changes of the load current after two additional rectifier loads are switched in, (b) the detection of harmonic distortions during this dynamic condition, and (c) the compensated power line current. The figure of (c) clearly demonstrates the adaptive capacity of the detection method developed in this thesis research.

4.5 Comparison With Conventional Detection Methods

To further demonstrate the effectiveness of the adaptive harmonic detection method, this section provides comparisons with two typical conventional detection methods: the instantaneous reactive power method and the synchronous detection method. The following power line conditions are used for the comparisons:

1. Harmonics from rectifier RL load
2. Harmonics from rectifier load with unbalanced single-phase loads
3. Harmonics from rectifier RL load with unbalanced line voltage
4. Harmonics from rectifier RLC load with unbalanced line voltage

4.5.1 Comparison Under Normal Power Line Voltage

1. *Harmonics from rectifier RL load*

When the load is balanced and when the power line voltage is normal, all three methods provide accurate detection results. This can be seen from Table 4.5 and the waveforms of compensated current in Figure 4.9, Figure B1, and Figure B2 in Appendix B. Table 4.5 shows that the current THD after compensation is reduced significantly to about 1% or less from 26%. And the compensated current waveforms are close to sinusoidal. This demonstrates that all three methods perform very well.

THD%		Before compensation	Adaptive harmonic detection	Instantaneous reactive power	Synchronous detection
Phase	A	26.07	1.05	0.51	0.36
	B	26.07	1.04	0.51	0.36
	C	26.07	1.05	0.50	0.36

Table 4.5: THD (%) of line current under rectifier RL load for three detection methods

2. *Harmonics from rectifier load with unbalanced single-phase loads*

When the load is unbalanced, the adaptive harmonic detection method and the instantaneous reactive power method provide accurate detection results. However, the performance of the synchronous detection method degrades. This can be seen from the waveforms and the THD values of the power line current compensated using these three methods. The waveforms for the adaptive harmonic detection method, the instantaneous reactive power method, and the

synchronous detection method are shown in Figure 4.12, Figure B3, and Figure B4 respectively. The THD values are listed in Table 4.6.

THD%		Before compensation	Adaptive harmonic detection	Instantaneous reactive power	Synchronous detection
Phase	A	22.61	3.98	4.87	6.41
	B	22.93	4.79	4.89	8.24
	C	22.84	4.64	4.86	8.07

Table 4.6: THD (%) of line current under unbalanced load for three methods

4.5.2 Comparison For Unbalanced Power Line Voltage Condition

When the power line voltage is unbalanced, the adaptive detection method performs well, but the instantaneous reactive power method performs poorly. The performance of the synchronous method varies depending on different loads. Two illustrating cases are given in the following.

1. *Harmonics from rectifier RL load*

Case 1 assumes the power line voltage is unbalanced and supplies a rectifier with RL load. Simulations are carried out to compare the performances of the three methods. Figure 4.10, Figure B5, and Figure B6 show the simulated results. The adaptive harmonic detection method performs well. On the other hand, both the instantaneous reactive power method and the synchronous detection method do not perform well, where the power line current is still distorted after compensation. Table 4.7 lists the THD values for the three methods.

THD%		Before compensation	Adaptive harmonic detection	Instantaneous reactive power	Synchronous detection
Phase	A	26.96	2.64	11.12	6.34
	B	25.01	2.39	11.30	7.09
	C	27.20	3.16	11.38	7.86

Table 4.7: THD (%) of rectifier RL load with unbalanced power line voltage

2. Harmonics from rectifier RLC load

Case 2 assumes the unbalanced power line voltage feeding a rectifier carrying a RLC load. The power line condition before compensation for this case is poorer than that for Case 1 as shown in Table 4.8. This table shows that the current THD before compensation for Case 2 has an average of 42.9%, while the average for Case 1 is 26.4%. The three methods are used to suppress the power line harmonic distortion. The waveforms of the compensated line currents for the adaptive detection method, the instantaneous reactive power method and the synchronous detection method are given in Figure 5.11, Figure B7 and Figure B8 respectively. The THD values of the compensated line current by the three methods are given in Table 4.8. This table shows that the performances of the three methods are similar to those in Case 1 where the adaptive harmonic detection method developed in this thesis performs well, but the other two methods do not perform well.

THD%		Before compensation	Adaptive harmonic detection	Instantaneous reactive power	Synchronous detection
Phase	A	44.58	2.76	11.46	6.38
	B	41.88	3.91	11.87	7.67
	C	42.20	2.86	11.93	8.53

Table 4.8: THD (%) of rectifier RLC load with unbalanced power line voltage

4.6 Concluding Remarks

This chapter, first, has presented a vigorous verification of the adaptive harmonic detection method developed in this thesis research using a square wave current of known harmonic distortion. Second, this chapter has verified the effectiveness of the adaptive detection method for steady state operations under typical power line conditions including line distortion caused by rectifier carrying different loads. Third, this chapter has verified the performance of the adaptive detection method for a dynamic operation where two additional rectifier loads are switched in. Fourth, this chapter has concluded that the adaptive detection method performs better than two well-known conventional detection methods particularly under abnormal power line conditions.

Chapter 5

Experimental Verification of Adaptive Harmonic Detection Method

This chapter shows the experimental verification of the adaptive harmonic detection method developed in this thesis research for the control of active power line filters. The adaptive method has been successfully implemented using state-of-the-art digital signal processor (DSP). This chapter presents the details of the hardware and the software implementations of the adaptive harmonic detection control. This chapter also presents four case studies: three for typical distorted power line conditions, and one for unbalanced power line condition. The objective of these case studies is to demonstrate the effectiveness of the adaptive harmonic detection method for both balanced and unbalanced distorted power line conditions. Experimental results and simulations are provided for the demonstration.

The following lists the sections in this chapter.

Section 5.1 presents the hardware implementation of the adaptive power line harmonic detection. This section describes both control circuit and power circuit implementations. This section also details the implementations in major components such as the TMS320LF2407 DSP from Texas Instruments and the 342GD120-316 Skiip converter module from Semikron.

Section 5.2 presents the software implementation of the adaptive detection. This section describes the software for data acquisition, harmonic detection, PWM control signals generation, etc. The flow chart of the software is given.

Section 5.3 presents the experimental verification of the adaptive harmonic detection method developed in this thesis research. This section provides experimental results and simulations for 4 case studies covering typical power line conditions.

Section 5.4 provides concluding remarks of this chapter.

5.1 Hardware DSP Implementation of Adaptive Harmonic Detection

This section describes the hardware DSP implementation of the adaptive harmonic detection method developed in this thesis research. The filter consists of two main parts: the first part is the control circuit mainly consisting of a digital signal controller, and the second part is the power circuit mainly consisting of a voltage-source power electronic inverter. The block diagram of the active filter is given in Figure 5.1.

5.1.1 Digital Signal Processor Control Circuit

The control circuit mainly consists of one DSP, two voltage sensors, four current sensors, and one interface circuit.

TMS320LF2407 DSP

The DSP board of TMS320LF2407 from Texas Instruments (TI) is used to implement the adaptive harmonic detection method for the control a power inverter to cancel the current harmonics from non-linear. The non-linear load used in the experiments is a three-phase ac-to-dc converter. The TI DSP has the following features:

- 16-bit fixed-point micro-controller
- ADC: 10-bit ± 1 , 500 ns conversion, 16-channel, analog-to-digital converter
- General-purpose bi-directional digital I/O
- PWM generator and 12 PWM output channels
- On board 7.3728-MHz oscillator for 30MIPS operating speed
- 64K onboard program/data memory RAM
- 32K on-chip Flash memory
- 0-3.3V input and output signals

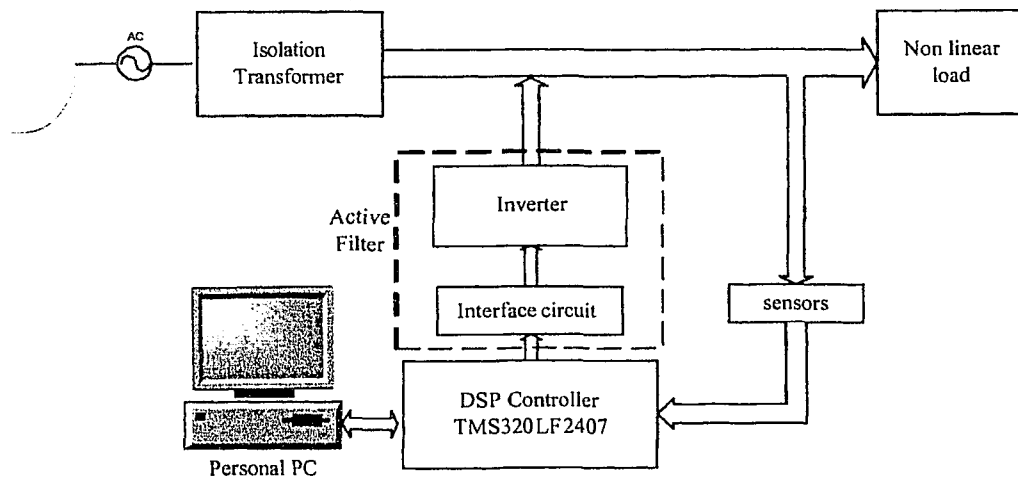


Figure 5.1: Block diagram of the active filter.

This 16-bit DSP computes the required harmonic compensation using the Q15 format that is the data is processed using 1 sign bit and 15 bits fraction representation. Eight of the 16 analog-to-digital converter channels are used to measure currents and voltages through current/voltage sensors: 2 channels for monitoring the load currents, 2 for the line voltages, 2 for the active filter output currents, and two for the line currents after filtering.

This TI DSP operates at 30 MHz clock frequency, and it generates switching signals for the inverter control using interrupts set at 15 kHz. The DSP uses the measured voltage and current waveforms to calculate the compensating currents required to cancel the load current harmonics. The DSP then generates switching signals through 6 general-purpose bi-directional digital I/O pins to control the power electronic inverter.

The block diagram of the DSP board is given in Figure 5.2. As shown in this figure, the currents and voltages are monitored by the DSP through P1 and P7. The switching signals are outputted from the DSP through P2 and P8 to the drive circuit of the power electronic inverter. The computer communicates through P9 with the DSP.

Voltage/current sensors and sensors-to-DSP interface

The waveforms of the line voltage and the load current are measured using voltage sensors and current sensors. The output range of the voltage sensors is ± 3.33 V for ± 100 V signals. The output range of the current sensors is ± 4 V for ± 10 A signals.

In order to match the 0-3.3V level of the input channel of DSP, operational amplifiers are used as sensor-to-DSP interface to convert the output range of the voltage sensor to 0-3.3V

for a $\pm 100V$ signal, and to convert the output range of the current sensor to 0-3.3 for a $\pm 10A$ signal.

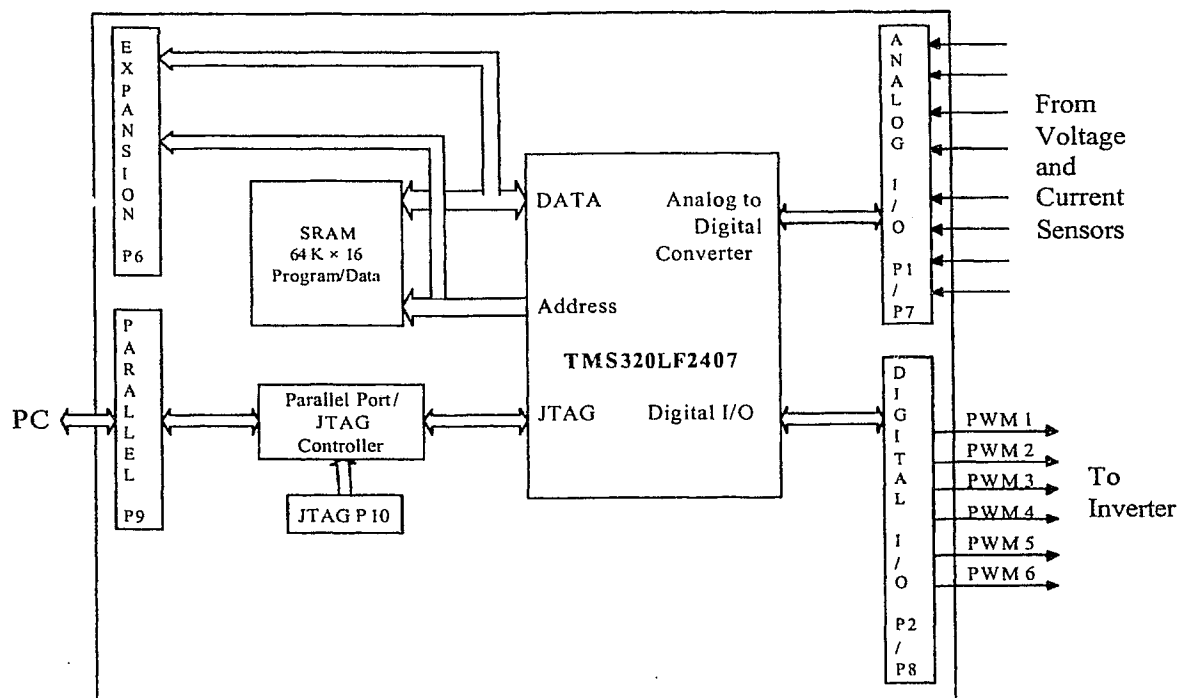


Figure 5.2: Block diagram of DSP TM320LF2407

DSP-to-inverter interface

The PWM channel in the DSP provides output signals of 3.3V. Since the IGBT switches in the inverter needs switching signals of 15V, a voltage-level shifter MC14504 is used as DSP-to-inverter interface to amplify the PWM output signals from the DSP to the inverter driver circuit.

5.1.2 Active Filter Power Circuit

A power electronic converter module Skiip® 342GD120-316 CTV from Semikron is used in the active filter circuit developed in this thesis research. This module is rated at 1200V and 300A. It consists of a rectifier, a capacitor, an inverter, and a driver. The rectifier is a three-phase full-bridge diode rectifier. The inverter is a three-phase standard bridge circuit using IGBT (insulated gate bipolar transistor) switches.

Non-linear rectifier load

The diode rectifier is disconnected from the Skiip module and is served as a non-linear load. The ac terminals of the rectifier are connected to the power line, and the dc terminals are connected to different loads.

Active filter inverter

The inverter, its driver and capacitor of the Skiip module is used as the power circuit of the active filter developed in this thesis. The rated current of the active filter was set to 10A for demonstration tests.

Isolation transformer and additional line distortion

For the convenience of performance the experiments in Ryerson Power Electronic Laboratory, the active filter is isolated from the utility power system using a transformer. The rating of this transformer is 23.4kVA, 208V and 28A. The impedance of this

transformer causes additional voltage distortion on the power line connecting the non-linear load. This results in a slightly more challenging line condition for testing the effectiveness of the active filter operation. This transformer is not needed in the practical implementation.

5.2 Software DSP Implementation of Adaptive Harmonic Detection

The adaptive control of the active filter developed in this thesis research has been implemented in software using the TMS320LF2407 DSP. Figure 5.3 shows the main parts of the active filter control software. The software is discussed in the following.

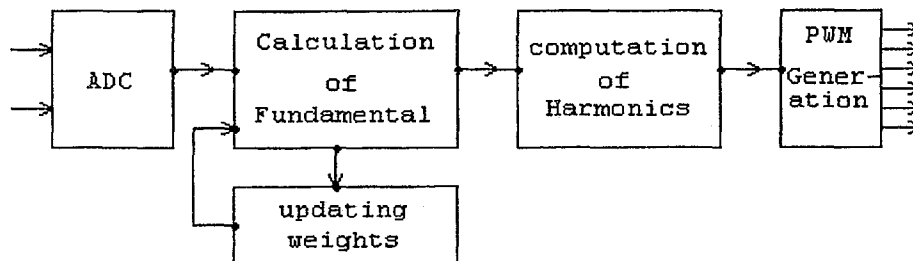


Figure 5.3: Block diagram of the software

5.2.1 Software Setting For Analog-to-digital Conversion

Software needs to be set up in the DSP for the conversion of analog signals (currents or voltages) into digital form before those signals can be processed by the DSP. The measured current and voltage signals are converted from analog to digital signals by the ADC unit in the DSP. The results of conversion are stored in 10-bit Result Registers as unsigned integers. Because the real signal can be positive and negative, the converted results need to be processed so that they can represent both positive and negative signals. This can be done by the following commands:

```
LACC      ADC_RESULT, 6      ; load ADC results into accumulator
XOR       #8000h          ; convert the results into Q15 format
```

The result is converted to the Q15 format (1 sign bit and 15 fraction bits) by XOR command. Therefore, the range of 0000h-03FFh for the Result Register is converted to a range of $-/+1$ in Q15 format.

5.2.2 Computation of Fundamental Power Line Current

Software is developed to compute the fundamental component of the power line current. The digital signals of the line voltage and current, after ADC conversion, are used to calculate the fundamental current. The calculation is carried out according to the adaptive noise cancellation algorithm. In this thesis, 5 weights are used in the adaptive filtering algorithm. Thus, 5 consecutive sampling points of voltage and current are needed. Three buffers are used to store the voltage and current samples and the values of the 5 weights. During each sampling period, the fundamental component is computed, and an error signal is obtained by subtracting the fundamental component from the measured power line current. At the end of each sampling period, the oldest sample point of voltage and current are discarded. Each of the remaining four sample points is moved to the next higher address in the buffer so that, at next sampling period, the newest sample point is stored in the top address of the buffer. This process can be illustrated using Figure 5.4.

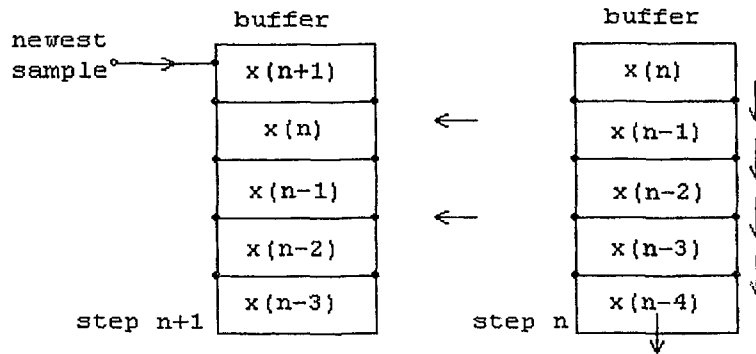


Figure 5.4: Diagram of buffer at step n and step n+1

5.2.3 Updating Weights For Adaptive Harmonic Detection

The weights are updated at each sampling period after the error signal is obtained. The updating is carried out according to the equation (3.1.21):

$$w_{l(k+1)} = w_{lk} + 2\mu E_k x_{k-l} \quad l = 0, 1, 2, 3, 4$$

The software uses indirect addressing mode to fetch the value of w_{lk} and x_{k-l} . There are 8 auxiliary registers (AR0-AR7) can be used for indirect addressing mode. This software uses AR2 for the addressing of w_{lk} , and AR3 for x_{k-l} . The content of AR2 is set to be the top address of the weight buffer, while AR3 is set to be the bottom address of the voltage buffer. Then the first new weight is calculated according to (3.2.21). After first calculation, the content of AR2 is increased by 1 and the content of AR3 decreased by 1. Then AR2 is pointing to the second value in the weight buffer, and AR3 is pointing to the second last value in voltage buffer. Thus, the second new value of weight is calculated. The process is repeated until AR2 points to the bottom address of the weight buffer and AR3 points to the top address of the voltage buffer.

The updated weights are stored to the weight buffer and are used to calculate the fundamental component in next sampling period. The old values of the weights are overwritten with the new ones. After the fundamental component is obtained, the harmonics can be calculated by subtracting the fundamental component from the measured power line current.

5.2.4 PWM Generation

The power line harmonics calculated using the method described above are used to generate the PWM signals. The TMS320LF2407 DSP has a built-in PWM generating function, which is controlled by the EV (event manager). The DSP has two event managers, EVA and EVB. These two event managers are exactly identical to each other in terms of functionality. For the sake of brevity, only the functionality of EVA is explained. Each EV contains the following functional blocks:

- Two general-purpose (GP) timers.
- Three compare units.
- Pulse-width modulation (PWM) circuits
- Dead-band generation units
- Interrupt logic

Each EV has two general-purpose timers. Each timer has a counter register, a 16-bit timer period register, and a 16-bit control register. The timer control register sets the counting mode, which can be one of the counting up mode and counting up/down mode. In this thesis, two methods for the generation of PWM inverter switching signals have been implemented

using Timer 1 of the EVA (event manager A) in the DSP. One is the standard triangular PWM, and the other is hysteresis comparison PWM.

For the generation of the triangular PWM switching signals, the counting up/down mode is used to produce a symmetrical triangular wave. The counter register stores the value of the counter and keeps increasing or decreasing depending on the direction of counting. The value in the period register determines the counting period, i.e. the period of the triangular waveform. This value also determines the switching frequency of the PWM. In this thesis research, the period register is set to 1500 to generate a 10kHz PWM switching frequency.

For the generation of the hysteresis comparison PWM signals, the counting up mode is used to set the period for each hysteresis comparison operation. This operation for generating PWM signals is simply by comparing the feedback current measured at the output of the active filter with the compensating current calculated using the adaptive harmonic detection algorithm developed in this thesis.

There are three compare units (compare units 1, 2, and 3) in the EV module. Each compare unit has a pair of PWM outputs. There are a total of 6 PWM outputs in the compare units. The harmonics of the 3-phases power line are stored in the 3 compare registers. The value of each compare register is constantly compared with the value of counter register of the general-purpose timer. In other words, the harmonics of each phase is constantly compared with the triangular waveform created by the general-purpose timer. When the values match, a transition (from low to high, or high to low) happens on the associated PWM outputs of the compare units. When a second match is made between the values, another transition (from high to low, or low to high) happens on the associated output. In this way, an output pulse is

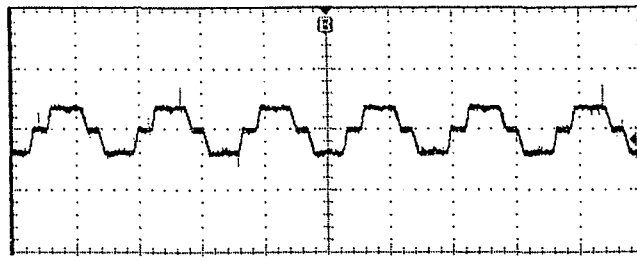
5.3 Experimental Verification of the Adaptive Harmonic Detection Method

This section presents the case studies for the verification of the adaptive harmonic detection method developed in this thesis research. The following provides the study, by DSP experiments and Simulink simulations, for 4 cases representing typical power line harmonic distortion conditions.

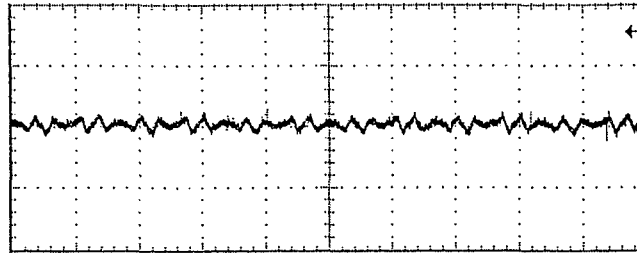
5.3.1 RL Rectifier Load (Case study 1: moderate power line harmonics)

Case study 1: In this case study, a diode rectifier carrying a RL load (30 Ω , 10 mH) is used as a source that injects harmonics on the three-phase power line of 110 V. This rectifier RL load is a typical moderate harmonics source found on the industrial power lines.

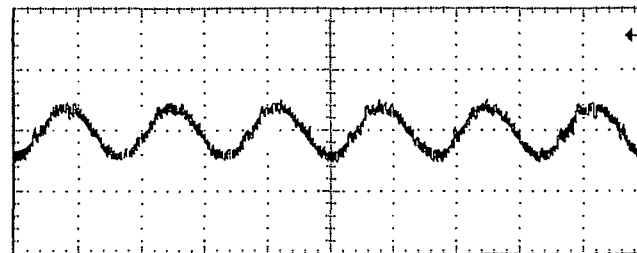
The experimental result for this case study is given in Figure 5.7. Part (a) of this figure shows the distorted power line current at the input of the rectifier. Part (b) shows the current harmonic distortion detected by the adaptive method developed in this thesis research with implementation in TMS320LF2407 DSP. Part (c) shows the current after compensation where the major lower harmonics are suppressed.



(a) Load current, 10A/div, 0.01s/div



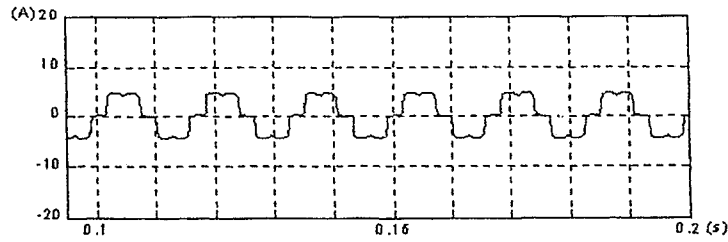
(b) Detected harmonic current, 10A/div, 0.01s/div



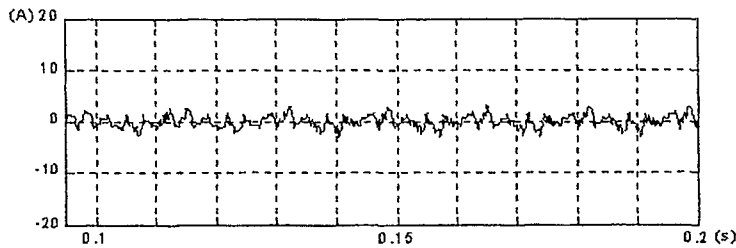
(c) Current after compensation, 10A/div, 0.01s/div

Figure 5.7 Experimental results for Case Study 1

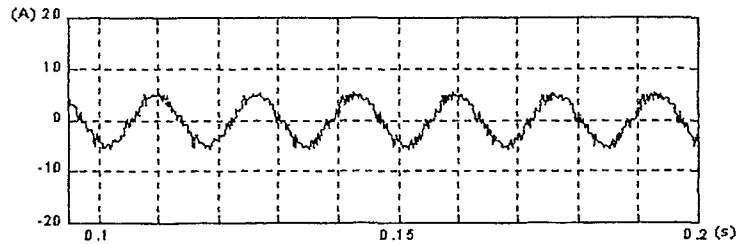
Figure 5.8 shows the computer simulation results. The simulation is implemented using the software Simulink, and the detection of the power line harmonic distortion uses the adaptive method developed in this thesis. This figure provides a convenient comparison with the experimental results in Figure 5.7. The THD of power line current before compensation is 26.17%, and the THD of the current after compensation is reduced to 9.02%.



(a) Simulated load current



(b) Detected harmonic current



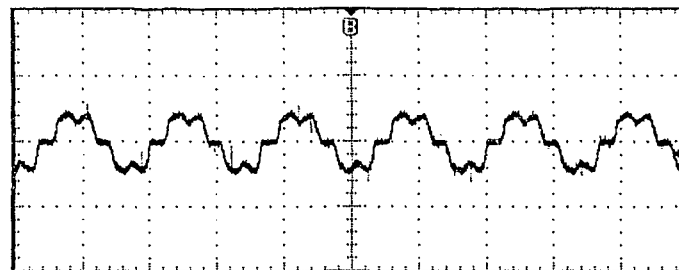
(c) Simulated current after compensation

Figure 5.8: Simulation results for Case Study 1.

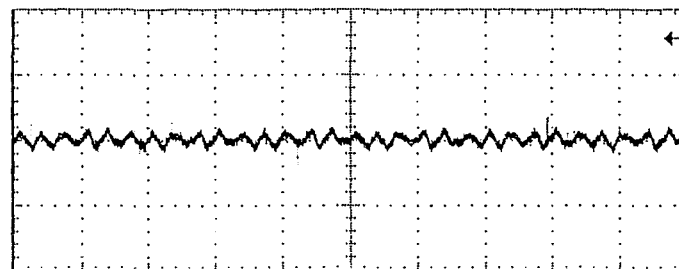
5.3.2 RLC Rectifier Load (Case study 2: more power line harmonics)

Case study 2: In this case study, the diode rectifier carrying a RLC load (30Ω , 2.5mH , $750\ \mu\text{F}$) is used as a source that injects harmonics on the three-phase power line. The input current harmonics content in this rectifier RLC load increases with the connection of the capacitor C , as compared with that in the RL rectifier load in Case study 1.

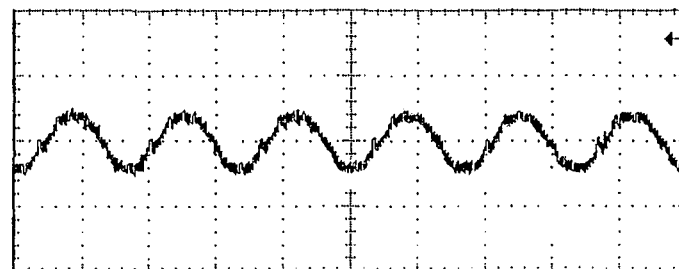
The experimental result for this case study is given in Figure 5.9. Part (a) of this figure shows the distorted power line current at the rectifier input. Part (b) shows the current harmonic distortion. Part (c) shows the current after compensation.



(a) Load current, 10A/div, 0.01s/div



(b) Detected harmonic current, 10A/div, 0.01s/div

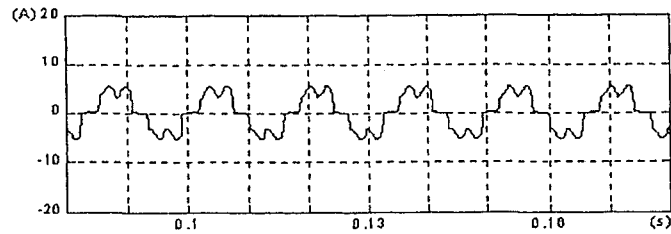


(c) Current after compensation, 10A/div, 0.01s/div

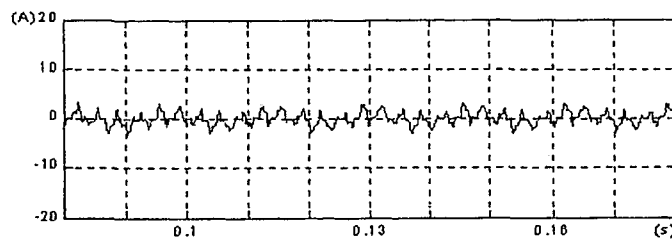
Figure 5.9: Experimental results for Case study 2

Figure 5.10 shows the computer simulation results using the software Simulink. This figure is provided for the comparison of the experimental results in Figure 5.9. The THD of power

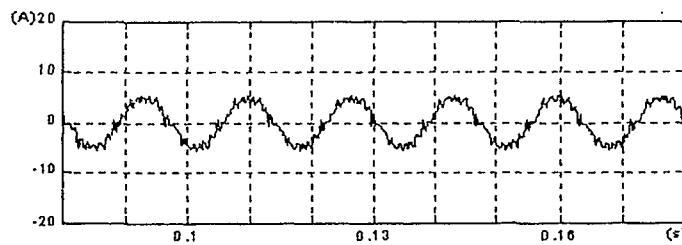
line current before compensation is 31.55%, and the THD of the current after compensation is reduced to 9.2%.



(a) Simulated load current



(b) Detected harmonic current



(c) Simulated current after compensation

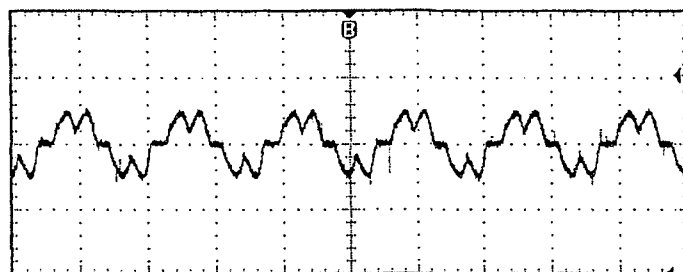
Figure 5.10: Simulation results for Case study 2.

5.3.3 RC Rectifier Load (Case study 3: increased power line harmonics)

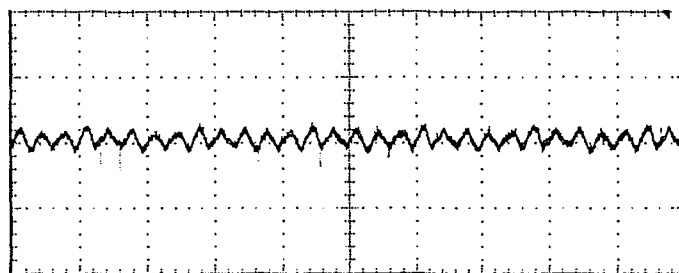
Case study 3: In this case study, the diode rectifier carrying a RC load (30Ω , $330 \mu\text{F}$) is used as a source that injects harmonics on the three-phase power line. The input current harmonics content in this rectifier RC load increases with the connection of the capacitor C

and without the connection of the inductor L, as compared with that in Case study 1 and Case study 2.

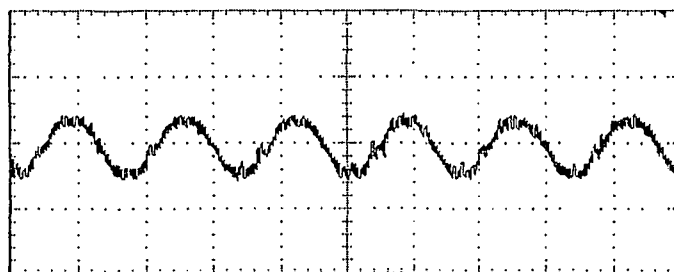
The experimental result for this case study is given in Figure 5.11. Part (a) of this figure shows the distorted power line current at the rectifier input. Part (b) shows the current harmonic distortion. Part (c) shows the current after compensation.



(a) Load current, 10A/div, 0.01s/div



(b) Detected harmonic current, 10A/div, 0.01s/div



(c) Current after compensation, 10A/div, 0.01s/div

Figure 5.11: Experimental results for Case study 3.

Figure 5.12 shows the computer simulation results using the software Simulink. This figure is provided for the comparison of the experimental results in Figure 5.11. The THD of power line current before compensation is 38.36%, and the THD of the current after compensation is reduced to 8.97%.

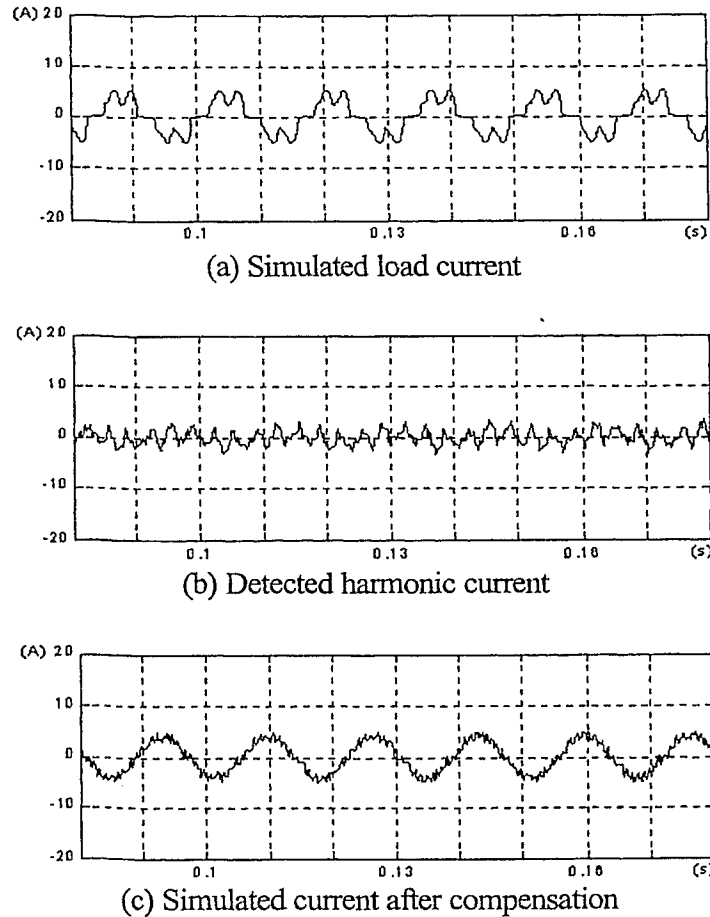


Figure 5.12: Simulation results for Case study 3.

5.3.4 Unbalanced Distorted Load (Case study 4: unbalanced power line harmonics)

Case study 4: This case study investigates the performance of the adaptive harmonic detection method in this thesis for the power line under an unbalanced and distorted loading

condition. This condition is established using a three-phase diode rectifier and a single-phase load connected between phase "b" and phase "c". The diode rectifier that causes power line distortion carries a load of 30Ω and 2.5mH , and the single-phase load that causes the unbalanced loading has a resistance of 40Ω .

The experimental result for this case study is given in Figure 5.12. Part (a) of this figure shows the distorted three-phase power line currents at the terminals of the combined rectifier load and the single load. This part clearly shows the unbalance on the three phases, where Phase "b" and Phase "c" draw more currents than Phase "a" does. Part (b) shows the current harmonic distortion. Part (c) shows the current after compensation.

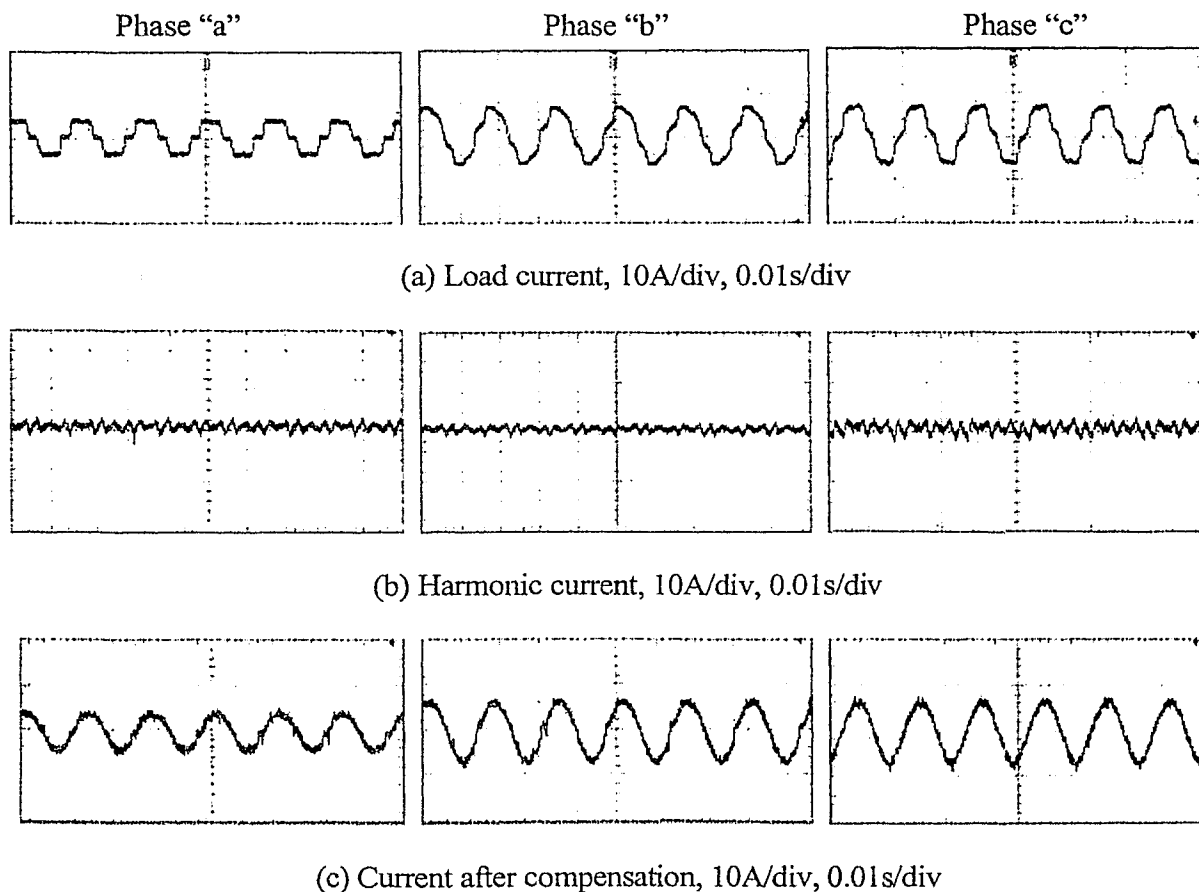


Figure 5.13: Experiment results for Case study 4.

Figure 5.14 shows the computer simulation results using the software Simulink for the unbalance loading condition. This figure is provided for the convenience of comparing the experimental results given in Figure 5.13.

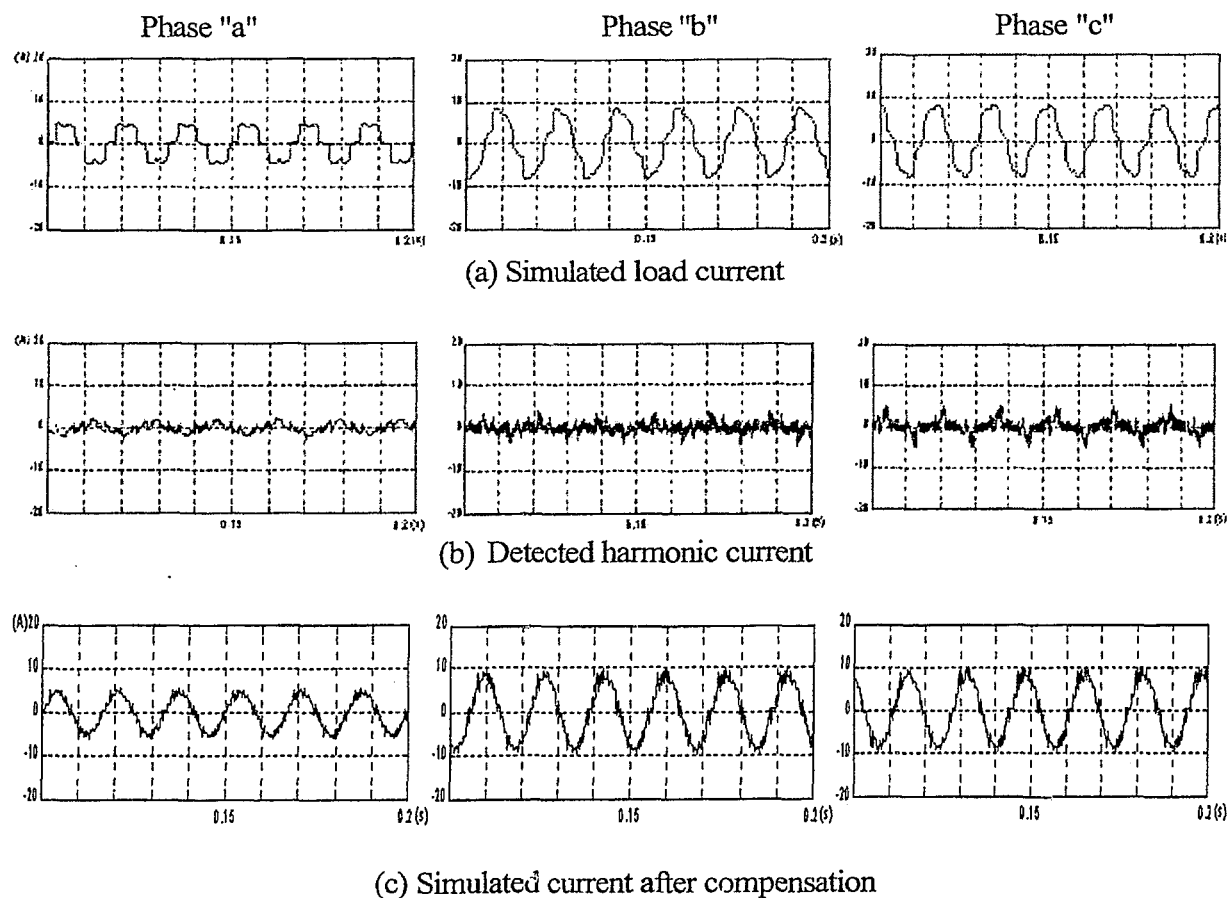


Figure 5.14: Simulation results for Case study 4.

5.4 Concluding Remarks

This chapter has presented the experimental verifications of the adaptive power line harmonic detection method developed in thesis research. The hardware and software

implementation of the adaptive harmonic detection has been detailed. The control implementation has been carried out using state-of-the-art digital signal processor.

Four case studies covering typical power line conditions have been carried out. Experimental results and simulations have been provided to demonstrate the effectiveness of the detection method developed in this thesis.

Chapter 6

Conclusions

6.1 Major Research Work Completed

The following presents a summary of the major tasks that has successfully completed to achieve the objective of this thesis research for the development of an advanced power line harmonic detection method for effective control of active filters.

- A. Extensive research has been conducted on active power line filtering operations. This includes studies of filter circuit configurations, filter control methods, real-time filter control algorithms, state-of-the-art control implementations, etc. In particular, a detailed study on conventional power line harmonic detection methods has been carried out. Also detection methods in areas outside the power electronics are studied. Based on the findings of these extensive research studies, a novel method for the active filter control based on noise cancellation theory has been found. This theory, which was originally developed for noise signal processing, has been applied by this thesis research for the control of power line active filters.

- B. Detailed formulations for the adaptive power line harmonic detection method have been developed. This method has been based on noise cancellation theory that was designed originally for the noise signal processing outside the area of power electronics. The original formulations for noise cancellation are considerably complex and complicated as compared with the common formulations encountered in the control of power electronics. Therefore, extensive research effort has been spent

first to fully understand all formulations for the original noise cancellation control, and second to significantly simplify the formulations for the control of power line active filters. Finally, a simple and practical formulation has been derived for filter control, and the formulation can easily be implemented in a digital signal processor.

- C. Vigorous verifications of effectiveness of the adaptive harmonic detection method have been carried out using computer simulations. First, this thesis research has verified the adaptive detection method using a square wave power line current of known harmonic distortion. Second, this thesis research has verified the effectiveness of the adaptive detection method for steady state operations under typical power line conditions including line distortion caused by rectifier carrying different loads. Third, this research has verified the performance of the adaptive detection method for dynamic operations such as switching in additional harmonic-rich rectifier loads. Fourth, this research has demonstrated that the adaptive detection method has performed better than two well-known conventional detection methods particularly under abnormal power line conditions.
- D. Experimental verifications of the adaptive harmonic detection method for the control of active power line filters have been conducted. This thesis research has demonstrated that the adaptive method has been successfully implemented using state-of-the-art digital signal processor. This research has designed the hardware and the software implementations of the adaptive detection control in details. This thesis has also presented four case studies: three for typical distorted power line conditions, and one for unbalanced power line condition.

6.2 Major Research Contributions

1. *An adaptive power line harmonic detection method* has been developed, which has been based on the findings of extensive research in the areas of inside and outside of power electronics controls.
2. *A simple and practical formulation of the adaptive harmonic detection method* has been developed, which has been simplified significantly from the original complex design formulations for noise cancellations.
3. *Vigorous verifications of effectiveness of the adaptive detection method using computer simulations* have been carried out, which have covered the steady state operations, the dynamic operations, normal power line conditions, non-ideal supply and loading conditions, etc.
4. *Experimental verifications of the accuracy of the adaptive detection method* have been conducted, which have covered typical distorted power line conditions for normal and unbalanced operations. As an illustration, this thesis has presented four experimental case studies: three for typical distorted power line conditions, and one for unbalanced power line condition.

6.3 Future Work

The following presents recommended future work on the power line active filtering operations.

- a. Carry out field tests of the adaptive power line harmonic detection method. The results given in this thesis are obtained in the Power Electronics Laboratory at Ryerson University. It is recommended to conduct the field tests in the industrial sites which have large power electronic motor drives.

- b. Improve the adaptive harmonic detection method based on the findings of the field tests.

- c. Eliminate the high orders of the power line harmonics. It is a common difficulty that active filters cannot easily eliminate the high-order power line harmonics without either operating at very high switching frequency or using a high-frequency passive filter.

Bibliography

- [1] L. Gyugi, E.C. Strycula, "Active AC Power Filter," Conf. Rec. of IEEE-IAS Annual Meeting, Oct. 1976, pp. 529-535
- [2] Luowei Zhou, Zicheng Li. "A Novel Active Power Filter Based on the Least Compensation Current Control Method," IEEE Trans. On Power Electronics, Vol. 15, No. 4, July 2000, pp. 655-659
- [3] Bhim Singh, Kamal Al-Haddad. "A review of Active Filters for Power Quality Improvement," IEEE Trans. On Industrial Electronics, Vol. 46, No. 5, Oct 1999, pp. 960-971
- [4] Tai Ling Leung, Sami Valiviita, Seppo J. Ovaska. "Adaptive and delayless Filtering System for Sinusoids with Varying Frequency," Southeastcon '99. Proceedings. IEEE , 25-28 March 1999, pp. 149 – 153
- [5] Hirofumi Akagi, Yoshihira Kanazawa, Akira Nabae. "Instantaneous Reactive Power Compensators Comprising Swithing Device without Energy Storage Components," IEEE trans. On Industry Applications, Vol. IA-20, No. 3, May/June 1984, pp 625-631
- [6] Chen, C.L., Lin, C.R., Huang, C.L.: "Reactive and Harmonic Current Compensation for Unbalanced Three-phase Systems Using the Synchronous detection Method," Elec. Power Syst. Res., 1993, 26, pp 163-170
- [7] S. Bhattacharya, A. Veltman, D. M. Divan, and R. D. Lorenz, "Flux based active filter controller," in Conf. Rec. IEEE-IAS Annu. Meeting, 1995, pp. 2483-2491.

- [8] M. Rastogi, N. Mohan, and A. A. Edris, "Filtering of harmonic currents, damping of resonances in power systems with a hybrid-active filter," in Proc. IEEE APEC'95, 1995, pp. 607-612.
- [9] W.M. Grady, M. Samotyj, A.H. Noyola, "Survey of Active Power line Conditioning Methodologies," IEEE Trans. On Power Delivery, vol. 5, No. 3, July, 1990, pp. 1526-1542
- [10] W.M. Grady, M. Samotyj, A.H. Noyola, "Improving Power Quality with Active Power Line Conditioners," First International conference on Power Quality, Paris France, Oct 1991, pp. 213-220
- [11] B. Widrow et al., "Adaptive Signal Processing," Printice Hall, Englewood Cliffs, N.J., 1985
- [12] Wang Qun; Wu Ning; Jiang Zejia: "An adaptive detecting approach of harmonic currents for active power filter," Power System Technology, 1998. Proceedings of POWERCON '98. 1998 International Conference, Vol. 2 , 18-21 Aug. 1998 pp:1528 - 1532
- [13] Fukuda, S.; Furukawa, Y.; Kamiya, H.: "An adaptive current control technique for active filters," Proceedings of the Power Conversion Conference, 2002. PCC Osaka 2002. vol. 2 , 2-5 April 2002. pp:789 - 794
- [14] Dastfan, A.; Gosbell, V.J.; Platt, D.: "Control of a new active power filter using 3-D vector control," IEEE Trans. on Power Electronics, Vol. 15, Issue: 1 , Jan. 2000 pp: 5 - 12
- [15] de Battista, H.; Mantz, R.J.: "Harmonic series compensators in power systems: their control via sliding mode," IEEE Trans on Control Systems Technology, Vol. 8 , Issue: 6 , Nov. 2000, pp: 939 - 947

- [16] Soares, V.; Verdelho, P.; Marques, G.D.: "An instantaneous active and reactive current component method for active filters," IEEE Transactions on Power Electronics, Vol. 15, Issue: 4, July 2000, pp:660 – 669
- [17] Fukuda, S.; Kamiya, H.: "Adaptive learning algorithm assisted current control for active filters," IEEE Conference Record of Industry Applications Conference, 36th IAS Annual Meeting, 2001, Vol. 1, 30 Sept.-4 Oct. 2001, pp:179 - 185 vol.1
- [18] J. G. Jiang, Q. Wang: "A Study of Harmonics Reduction, detection and Evaluation," IEEE Proceedings of the 3rd World Congress on Intelligent Control and Automation, June 28- July 2, 2000, Hefei, China, pp. 3759-3760
- [19] Jou, H.-L.: "Performance comparison of the three-phase active-power-filter algorithms," IEE Proceedings of Generation, Transmission and Distribution, Vol. 142, Issue: 6, Nov. 1995, pp:646 – 652
- [20] M. El-Habrouk, M.K. Darwish, P. Mehta: "Active power filter:; A review," IEE Proc,- Electr. Power Appl., Vol. 147, No. 5, Sept. 2000
- [21] H.Akagi, A. Nabae, and S. Atoh, "Control strategy of active power filters using multiple voltage-source PWM converters," IEEE Trans. Ind. Appl., vol. IA-22, no.3, pp. 460, 1986.
- [22] H.Akagi, F.Z. Peng, A.Nabae, "A Study of active power filters using quad-series Voltage-Source PWM Converters for Harmonic Compensation ," IEEE Trans. Power Electron., vol.5, no.1, pp.9, 1990.
- [23] A.Cavallini, G.C.Carlo, "Compensation Strategies for Shunt Active filter control", IEEE Trans. Power Electron., vol. 9, no. 6, pp. 587, 1994.

- [24] Vasco Soares, P.Verdelho, and G.D.Marques, "An Instantaneous Active and Reactive Current Component Method for Active Filters", IEEE Trans. Power Electron.,vol.15,no.4, pp.660, 2000

- [25] S-J Huang, J-C wu, "A Control Algorithm for Three-Phase Three-wired Active Power Filters Under Nonideal Mains Voltages", IEEE Trans. Power Electron.,vol.14, no.4, pp.753, 1999.

- [26] L.A.Moran, Juan W. Dixon, R.R.Wallace, "A Three-Phase Active Power Filter Operating with Fixed Switching Frequency for Reactive Power and Current Harmonic Compensation", IEEE Trans. Ind. Electron., vol.42, no.4, pp.402, 1995

- [27] L.Benchatia, S.Saadate and A.Salem nia. "A Comparison of Voltage Source and Current Source Shunt Active Filter by Simulation and Experimentation", IEEE Trans. Power Systems, vol. 14, no. 2. pp.642 , 1999.

- [28] Juan W.Dixon, J.J.Garcia, and Luis Moran, "Control System for Three-Phase Active Power Filter Which Simultaneously Compensates Power Factor and Unbalanced Loads", IEEE Trans.Ind. Electron.,vol.42, no.6, pp.636, 1995

- [29] J.Sebastian Tepper, Juan W.Dixon, G.Venegas, and Luis Moran, "A Simple Frequency-Independent Method for Calculating the Reactive and Harmonic Current in a Nonlinear Load", IEEE Trans. Ind. Electron., vol.43.,no.6, 1996

- [30] C.K.Duffey, Ray P. Stratford, "Update of Harmonic Standard IEEE-519: IEEE Recommended Practices and Requirements for Harmonic Control in Electric Power Systems", IEEE Trans. Ind.Appli.,vol.25, no.6,nov/dec., 1989

- [31] SIMULINK-Dynamic System Simulation for MATLAB[®] , Using SIMULINK Version 2 ., The Mathworks Inc.1997

- [32] N.Mohan, T.M.Undeland and W.P.Robbins, "Power Electronics- converters, applications, and design", 2nd edition John Wiley & Sons, New York.
- [33] G. Ledwich, P. Doulai, "Multiple Converter Performance and Active Filtering," IEEE Tran. On Power Electronics, Vol. 10, No. 3, May 1995, pp. 273-279
- [34] S. Fukuda, T. Endoh, "Control Method for a Combined Active Filter System Employing a Current Source Converter and a High Pass Filter," IEEE Industry Applications, Vol. 31, No. 3, May/June 1995, pp. 590-597
- [35] H. Akagi, "Trends in Active Power Line Conditioners," IEEE Trans. On Power Electronics, Vol. 9, No. 3, May 1994, pp 263-268
- [36] A. Flemming, D. Alain, "Adjustable Speed Drive with Active Filtering Capability for Harmonic Current Compensation," IEEE PESC, Vol. II, 1995, pp. 1137-1143.

Appendix A

Simulation Models for Two Conventional Detection Methods

This appendix presents two Simulink models: one for the instantaneous reactive power detection method for the control of active filters, and one for the synchronous detection method.

1 Simulink model of instantaneous reactive power method

Figure A1 illustrates the Simulink model of instantaneous reactive power method. Inputs 1, 2, 3 are 3-phase power line voltages, input 4, 5, 6 are the 3-phase load currents. Output1 is shown as p in Figure A1. It is the ac component of the real power p_{ac} . Output2 is shown as q in Figure A1. It is the ac component of imaginary power q_{ac} . In this model, a low-pass filter has been used as required by the method to extract p_{ac} and q_{ac} .

2 Simulink model of synchronous detection method

Figure A2 shows the Simulink model for the synchronous detection method. Input 1, 2, and 3 are the 3-phase power line voltages, and input 4, 5, and 6 are 3-phase load currents. Output 1, 2, and 3 are the harmonics calculated by the synchronous detection method. A low-pass filter is used as required by the method to obtain the average power P_{dc} .

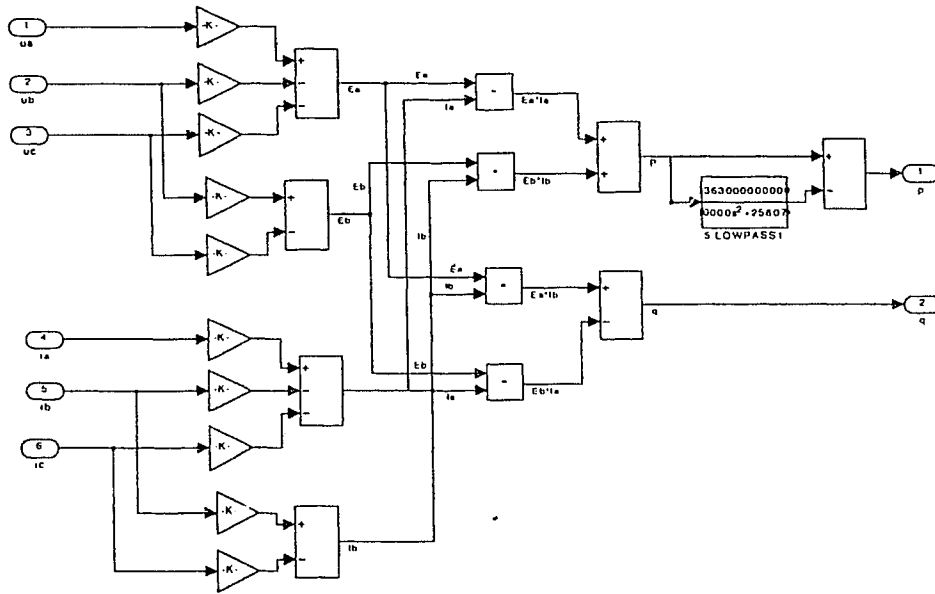


Figure A1: Model of instantaneous reactive power method

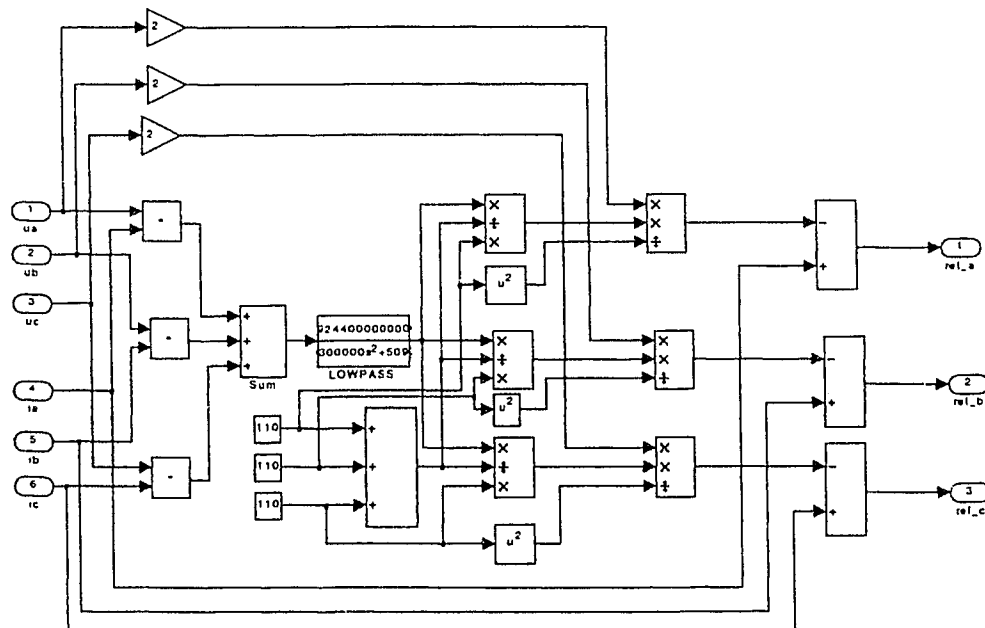


Figure A2: Model of synchronous detection method

Appendix B

Simulation Results of Two Conventional Detection Methods

This appendix presents the simulation results of the instantaneous reactive power method and the synchronous detection method. The results are presented as follows:

- 1 Harmonics from rectifier RL load
- 2 Harmonics from rectifier load with unbalanced single-phase loads
- 3 Harmonics from rectifier RL load with unbalanced line voltage
- 4 Harmonics from rectifier RLC load with unbalanced line voltage

1. Harmonics from rectifier RL load

Instantaneous reactive power method

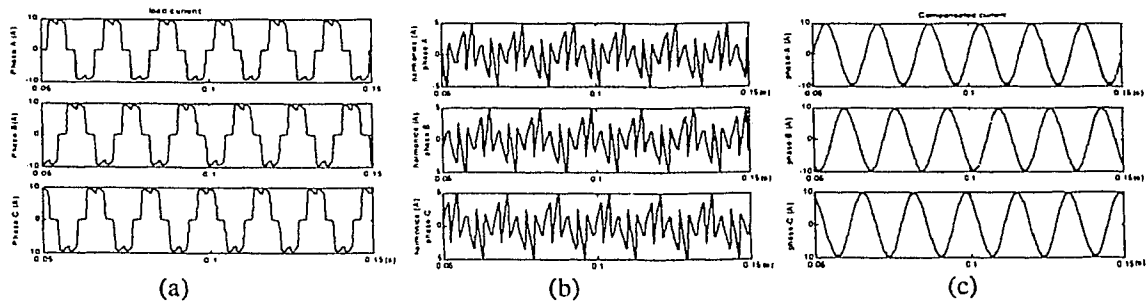


Figure B1: Detection results of rectifier RL load using instantaneous reactive power method

Figure B1 (a) shows the power line current before compensation.

Figure B1 (b) shows the detected harmonics using instantaneous reactive power method.

Figure B1 (c) shows the current after compensation.

Synchronous detection method

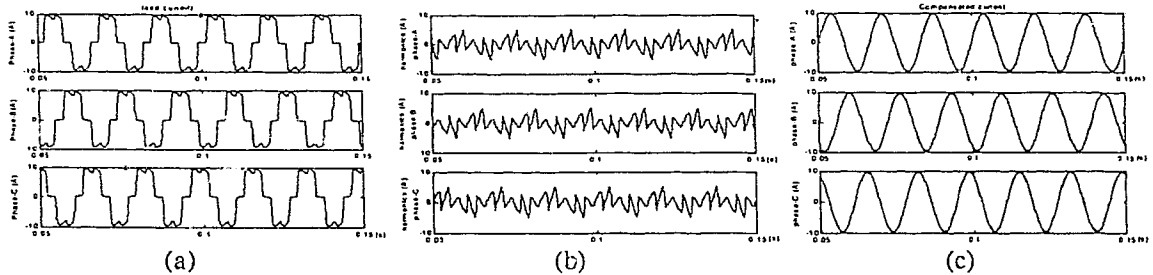


Figure B2: Detection results of rectifier RL load using synchronous detection method

Figure B1 (a) shows the power line current before compensation.

Figure B2 (b) shows the detected harmonics using synchronous detection method.

Figure B2 (c) shows the current after compensation.

2 Harmonics from rectifier load with unbalanced single-phase loads

Instantaneous reactive power method

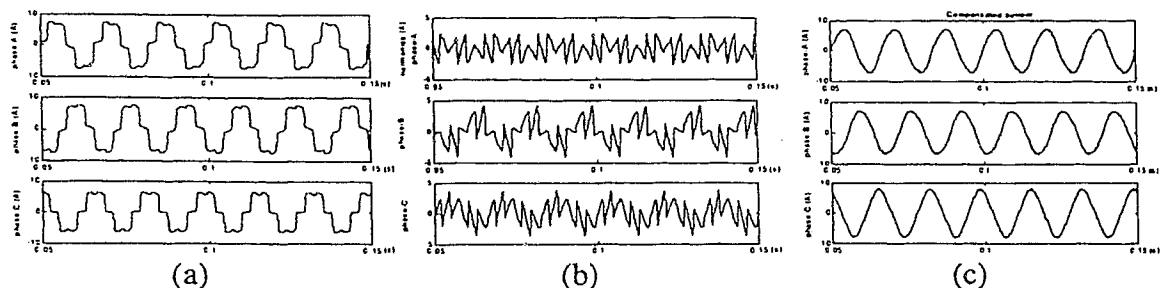


Figure B3: Detection results of unbalanced load using instantaneous reactive power method

Figure B3 (a) shows the power line current before compensation.

Figure B3 (b) shows the detected harmonics using instantaneous reactive power method.

Figure B3 (c) shows the current after compensation

Synchronous detection method

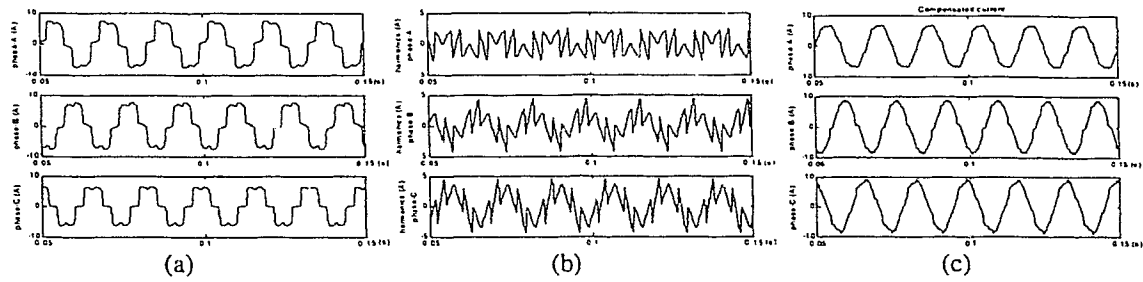


Figure B4: Detection results of unbalanced load using synchronous detection method

Figure B4 (a) shows the power line current before compensation.

Figure B4 (b) shows the detected harmonics using synchronous detection method.

Figure B4 (c) shows the current after compensation.

3. Harmonics from rectifier RL load with unbalanced line voltage

Instantaneous reactive power method

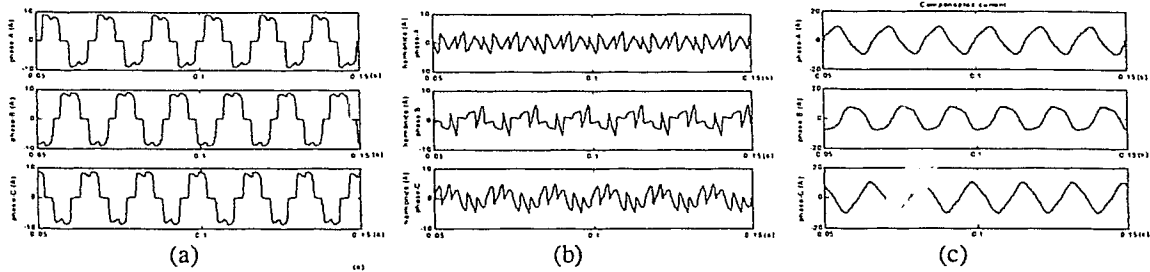


Figure B5: Detection results of rectifier RL load using instantaneous reactive power method with unbalanced power line voltage

Figure B5 (a) shows the power line current before compensation.

Figure B5 (b) shows the detected harmonics using instantaneous reactive power method.

Figure B5 (c) shows the current after compensation.

Synchronous detection method

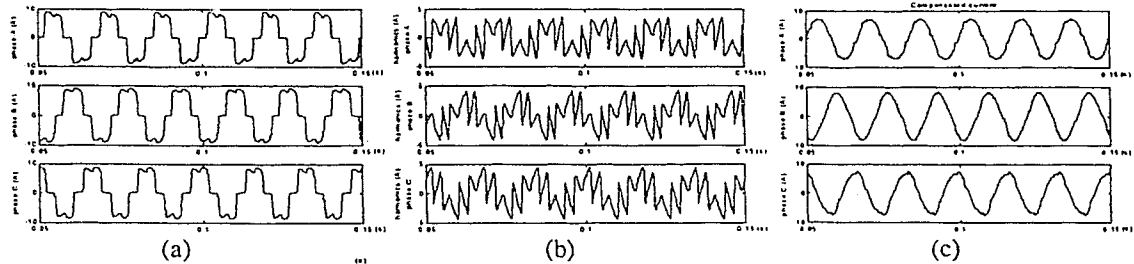


Figure B6: Detection results of rectifier RL load using synchronous detection method with unbalanced power line voltage

Figure B6 (a) shows the power line current before compensation.

Figure B6 (b) shows the detected harmonics using synchronous detection method.

Figure B6 (c) shows the current after compensation.

4. Harmonics from rectifier RLC load with unbalanced line voltage

Instantaneous reactive power method

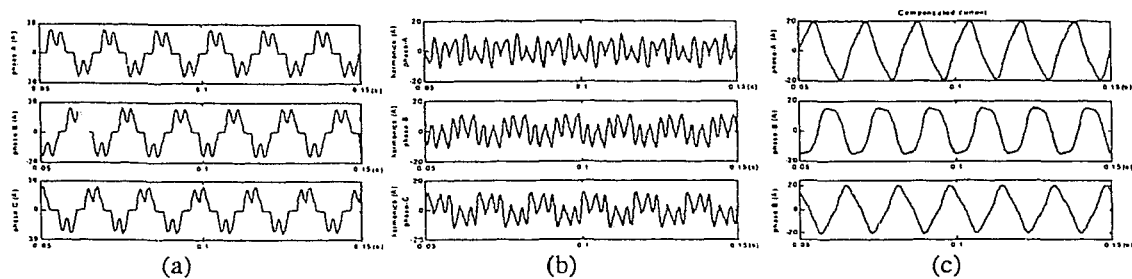


Figure B7: Detection results of rectifier RLC load using instantaneous reactive power method with unbalanced power line voltage

Figure B7 (a) shows the power line current before compensation.

Figure B7 (b) shows the detected harmonics using instantaneous reactive power method.

Figure B7 (c) shows the current after compensation.

Synchronous detection method

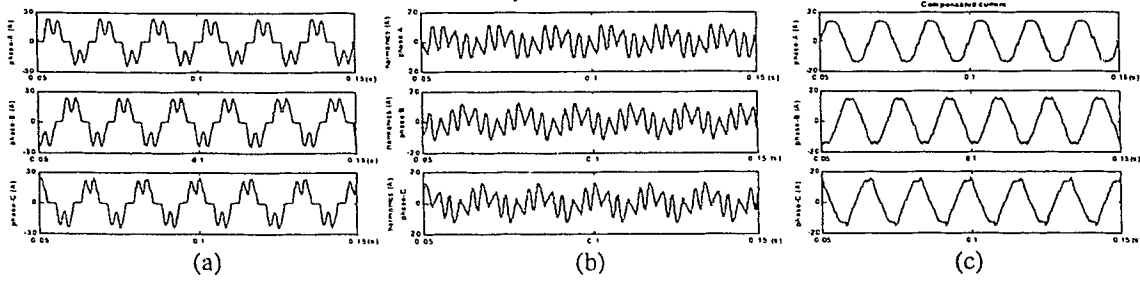


Figure B8: Detection results of rectifier RLC load using synchronous detection method with unbalanced power line voltage

Figure B8 (a) shows the power line current before compensation.

Figure B8 (b) shows the detected harmonics using synchronous detection method.

Figure B8 (c) shows the current after compensation.

Appendix C

DSP Software Codes for Adaptive Harmonic Detection Method

This appendix lists the DSP codes for adaptive harmonic detection method. The codes are composed using assembly language.

1. Software module "tstvec.asm"

```
*****
;
; FILENAME:          tstvec.asm
; DESCRIPTION:       Sets the interrupt vector address and
;                   includes Vector needed for real time applications
;
; STATUS:           Aug, 20, 2004
; By:              Weidong Liu
;
*****
.include          "c200mnr.i" ; Include conditional assembly options.
.mmregs          ; Include standard register mnemonics.
;
; GLOBAL DECLARATIONS
;
*****
.global _c_int0, PHANTOM, T1_ISR, NMI_ISR

;
*****
; This is the vectors table, to be located at 0x0000@prog.
;
*****
.sect "vectors"

RESET  B    _c_int0          ;00
INT1   B    PHANTOM         ;02
INT2   B    T1_ISR          ;04
INT3   B    PHANTOM         ;06
INT4   B    PHANTOM         ;08
INT5   B    PHANTOM         ;0A
INT6   B    PHANTOM         ;0C

.if ( 1 ) ; macro occupies fourteen words in the vector table.
MON_EINTR mon_eintr_vecs
.else ; macro not in vector table.
MON_EINTR_B B MON_EINTR
```

```
HUNG10    B    HUNG10
HUNG12    B    HUNG12
HUNG14    B    HUNG14
HUNG16    B    HUNG16
HUNG18    B    HUNG18
HUNG1A    B    HUNG1A
    .endif
```

```
HUNG1C    B    HUNG1C
HUNG1E    B    HUNG1E
HUNG20    B    HUNG20
TRAP      B    TRAP
NMI       B    NMI_ISR
```

```
.if( 1 )
```

;macro occupies eight words in the vector table.

```
MON_ETRAP mon_etrap_vecs
```

```
.else ; macro not in vector table.
```

```
MON_ETRAP_B B    MON_ETRAP
```

```
HUNG28    B    HUNG28
```

```
HUNG2A    B    HUNG2A
```

```
HUNG2C    B    HUNG2C
```

```
.endif
```

```
HUNG2E    B    HUNG2E
```

```
HUNG30    B    HUNG30
```

```
HUNG32    B    HUNG32
```

```
HUNG34    B    HUNG34
```

```
HUNG36    B    HUNG36
```

```
HUNG38    B    HUNG38
```

```
HUNG3A    B    HUNG3A
```

```
HUNG3C    B    HUNG3C
```

```
HUNG3E    B    HUNG3E
```

```
.end
```

2. Assembly code linker command file

```
/*
 * Filename: tst2adf2.cmd
 * Author: Weidong Liu, Ryerson University
 * Last Modified: Aug, 20, 2004
 * Description: Assembly code linker command file for LF2407 DSP.
 */
```

MEMORY

```
{
  PAGE 0: /* Program Memory */
  VECTOR: org=00000h, len=00040h /* vectors */
  PROG:   org=00040h, len=07FBCh /* ext mem */
  B0:    org=0FF00h, len=0100h /* CNF=1 */

  PAGE 1: /* Data Memory */
  MMRS : origin = 0h , length = 05Fh /* MMRS */
  B2 : origin = 0060h , length = 020h /* DARAM */
  B0B1 : origin = 0200h , length = 0200h
  SARAM : origin = 0800h , length = 0800h
  DATA : origin = 8000h , length = 8000h /* EMIF */
}
```

SECTIONS

```
{
  .text: > PROG PAGE 0
  .data: > PROG PAGE 0
  .bss: > B0B1 PAGE 1
  vectors: > VECTOR PAGE 0 /* interrupt vectors */
  stack: > SARAM PAGE 1 /* stack */
  sincos: > B0B1 PAGE 1 /* sine variables */
  data_log: > B0B1 PAGE 1 /* data log space */
  vari: > B0B1 PAGE 1 /* parameters */
  pid_reg1: > B0B1 PAGE 1 /* PI control */
  mon_main: > PROG PAGE 0 /* Main Mon */
  mon_pge0: > B2 PAGE 1 /* Used by RT monitor*/
  mon_rgst: > B2 PAGE 1 /* Used by RT monitor*/
}
```

3. Main routine and ISR (Interrupt service routine)

```

*****
* Filename:      main3.asm
* Author:       weidong liu
* Last Modified: Aug, 20, 2004
* Description:  System and buffers initialization
*              ADC, PWM, and interrupt setup
*****

    .include     "x24x_app.h"

    .global     _c_int0, T1_ISR, PHANTOM, NMI_ISR
               .global MON_RT_CNFG

    .ref        DATA_LOG, DATA_LOG_INIT
    .ref        dlog_iptr1, dlog_iptr2
    .ref        trig_value
;~~~~~
;Constant definitions
;~~~~~
d            .set 150           ;delay 4.95us
P_num       .set 0005h        ;number of sampling points
sample_TP   .set 2000        ;sampling frequency (2000-->15KHz)
half_sampl  .set 750         ;half of the period
mio_a       .set 0200h        ;performance factor Q15, range 0-1
mio_b       .set 0200h        ;performance factor Q15, range 0-1
;~~~~~
;Uninitialized global variable definitions
;~~~~~
w_coeffa    .usect "vari", P_num ;weights of adapter,a
w_coeffb    .usect "vari", P_num ;weights of adapter,b
vltg_a      .usect "vari", P_num ;phase a voltage
vltg_b      .usect "vari", P_num ;phase b voltage
load_ia     .usect "vari", 1     ;phase a load current
load_ib     .usect "vari", 1     ;phase b load current
cmp_ia      .usect "vari", 1     ;phase a compensating current
cmp_ib      .usect "vari", 1     ;phase b compensating current
cmp_ic      .usect "vari", 1     ;phase c compensating current
fund_comp_a .usect "vari", 1     ;fundamental component, phase a
fund_comp_b .usect "vari", 1     ;fundamental component, phase b
fund_comp_c .usect "vari", 1     ;fundamental component, phase c
;out_adpt_a .usect "vari", 1     ;adapter output, phase a
;out_adpt_b .usect "vari", 1     ;adapter output, phase b
;out_adpt_c .usect "vari", 1     ;adapter output, phase c
err_a       .usect "vari", 1     ;harmonics, phase a

```

```

err_b      .usect      "vari", 1      ;harmonics, phase b
err_c      .usect      "vari", 1      ;harmonics, phase c
mio_err_a  .usect      "vari", 1      ;2*mio*e(k) in weights update
mio_err_b  .usect      "vari", 1      ;2*mio*e(k) in weights update
templ      .usect      "vari", 1      ;general purpose variable
sign       .usect      "vari", 1
norm       .usect      "vari", 1
ia_gain    .usect      "vari", 1
ia_offset  .usect      "vari", 1
ib_gain    .usect      "vari", 1
ib_offset  .usect      "vari", 1
cmpa_gain  .usect      "vari", 1
cmpa_offset .usect      "vari", 1
cmpb_gain  .usect      "vari", 1
cmpb_offset .usect      "vari", 1
ua_gain    .usect      "vari", 1
ua_offset  .usect      "vari", 1
ub_gain    .usect      "vari", 1
ub_offset  .usect      "vari", 1

```

```

      .text
      _c_int0:
;=====
;Macro defining
;=====
delay .MACRO          ;set the delay time
      .loop d
      NOP
      .endloop
      .ENDM

initia .MACRO      addr
      LAR          AR1, #addr ;initializing data buffer
      LDP          #addr    ;to '0s' of phase a voltage
      MAR          *, AR1
      .loop        P_num
      SPLK         #0000h, *+
      .endloop
      .ENDM

;-----
;macro for moving data in voltage buffer:
; voltage result is stored in the buffer, the old data are move
; to next higher address, so the lastest
; data is always stored in the first location of the buffer
;-----
mov .MACRO      addr1

```

```

MAR      *, AR0
LAR      AR0, #addr1      ;AR0 as the pointer
LDP      #templ
SAR      AR0, templ      ;store AR0 to templ
LACC     templ
ADD      #P_num          ;point to the bottom of the buffer
SUB      #2              ;move starts at
                          ;the second last data address

SACL     templ
LAR      AR0, templ
LDP      #addr1
.loop    P_num-1
DMOV     *-,             ;every data is copied to next location
.endloop
.ENDM

```

```

-----
;Macro for fundamental computation
-----
;

```

```

Fund     MACRO          v, w, f
        LAR            AR2, #v
        LAR            AR3, #w
        LACC #0
        SPM            1
        .loop P_num    ;COMPUTE X*W
        LDP            #v
        MAR            *, AR2
        LT             *+, AR3
        LDP            #w
        MPY            *+
        APAC
        .endloop
        SPM            0
        LDP            #f
        SACH f
        .ENDM

```

```

~~~~~
;Configure the System Control and Status Registers
~~~~~
;

```

```

POINT_PG0
CLRC     SXM            ;Clear Sign Extension Mode
SETC     OVM
CLRC     CNF            ;Config Block B0 to Data memory.
SPM      0

```

```

;~~~~~
;initializing data buffer
;~~~~~
    initia    vltg_a
    initia    vltg_b
    initia    w_coeffa
    initia    w_coeffb
    LDP       #ia_gain
    SPLK      #1FFFh, ia_gain           ;Q13
    SPLK      #0000h, ia_offset        ;Q15
    SPLK      #21F0h, ib_gain          ;Q15
    SPLK      #0100h, ib_offset        ;Q15
    SPLK      #1FFFh, ua_gain          ;Q13
    SPLK      #0280h, ua_offset        ;Q15
    SPLK      #1F3Fh, ub_gain          ;Q13
    SPLK      #0200h, ub_offset        ;Q15
    SPLK      #1FFFh, cmpa_gain        ;Q13
    SPLK      #0000h, cmpa_offset      ;Q15
    SPLK      #1FFFh, cmpb_gain        ;Q13
    SPLK      #0000h, cmpb_offset      ;Q15
;=====
;set configuration registers
;=====
    POINT_PF1
    SPLK      #0085h, SCSR1           ; with 4X clock=30MHz
    LACC      SCSR2
    OR        #0000000000001011b
    AND       #0000000000001111b
    SACL      SCSR2
;~~~~~
;Disable the watchdog
;~~~~~
    POINT_PF1
    SPLK      #0000000011101000b, WDCR
    LDP       #templ
    SPLK      #0000000001000000b, templ
    OUT       templ, WSGR
;~~~~~
;Configure I/O pins
;~~~~~
    POINT_PF2
    SPLK      #0000111111000000b, MCRA ;set 6 PWM outputs
    SPLK      #1111111100000000b, MCRB
    SPLK      #0000h, MCRC

```

```

sik_len      .set      100                                ;setup the software stack
stk          .usect   "stack", stk_len
;~~~~~
;Configure timer1 AND PWM
;~~~~~
POINT_EV
SPLK #0000h, T1CON                                ;RESET CONTROL REGISTERS
SPLK #0000h, T2CON
SPLK #0000h, GPTCON
SPLK #0000h, T1CNT
SPLK #sample_TP, T1PER
SPLK #0000000000000000b, ACTR                    ;6 PWM forced-low initially
SPLK #0000101000000000b, COMCON                 ;load ACTR immediately
                                                ; compare action disabled
SPLK #1001000001000000b, T1CON                 ;enable timer1, counting up mode
;~~~~~
;setup ADC
;~~~~~
POINT_PF2
SPLK #0100000000000000b, ADCL_CNTL1            ;reset ADCTRL1
SPLK #0010000000010000b, ADCL_CNTL1            ;Cascd, start-stop mode
SPLK #5, MAXCONV                                 ;set ADC conversion order
SPLK #6420h, CHSELSEQ1
SPLK #00A8h, CHSELSEQ2
SPLK #0000h, CHSELSEQ3
SPLK #0, CALIBRATION
LAR AR7, #stk                                    ;point to stack
CALL DATA_LOG_INIT                             ;initialize parameter display function
;~~~~~
;setup core interrupts
;~~~~~
POINT_PGO
SPLK #0000h, IMR
CALL MON_RT_CNFG                                ;call realtime monitor routine
LACC IFR
SACL IFR
SPLK #0000000001000010b, IMR                   ;enable INT2 and 7
POINT_EV
SPLK #0FFFFh, EVAIFRA                           ;setup the event manager interrupts
SPLK #0FFFFh, EVAIFRB
SPLK #0FFFFh, EVAIFRC
SPLK #0080h, EVAIMRA                             ;enable timer1 period int
SPLK #0000h, EVAIMRB
SPLK #0000h, EVAIMRC
POINT_EVB
SPLK #0FFFFh, EVBIFRA

```

```

SPLK #0FFFFh, EVBIFRB
SPLK #0FFFFh, EVBIFRC
SPLK #0000h, EVBIMRA
SPLK #0000h, EVBIMRB
SPLK #0000h, EVBIMRC
CLRC INTM ;enable global interrupt
;=====
;main code
;=====
loop
    B    loop

*****
* Interrupt service routine T1_ISR
* Description: In this ISR, the following functions are implemented
* - ADC conversion
* - Adaptive algorithm
* - PWM generation
*****
T1_ISR:
    SETC    SXM
    POINT_ PG0 ;Context saving
    MAR     *,AR7 ;AR7 is stack pointer
    MAR     *+ ;skip one position
    SST     #1, *+ ;save ST1
    SST     #0, *+ ;save ST0
    SACH    *+ ;save acc high
    SACL    * ;save acc low
    POINT_EV ;clear EVA interrupt flag
    LACC    EVAIFRA ;clear EVA interrupt flag
    SACL    EVAIFRA
    mov     vltg_a ;move voltage buffer
    mov     vltg_b

;=====
; load current conversion of phase a
;=====
    POINT_PF2
    LACC    ADC_RESULT0, 6
    XOR     #8000h
    LDP     #templ
    SACL    templ
    LT     ia_gain ;ia_gain in Q13
    MPY    templ ;Q13 x Q15 = Q28
    PAC
    ADD     ia_offset,13 ;add offset in Q28

```

```

LDP      #load_ia
SACH    load_ia,3          ;Convert final result to Q15

```

```

;=====  

; load current conversion of phase B  

;=====  


```

```

POINT_PF2
LACC    ADC_RESULT1, 6
XOR     #8000h
LDP     #templ
SACL    templ
LT      ib_gain           ;ib_gain in Q13
MPY     templ            ;Q13 x Q15 = Q28
PAC
ADD     ib_offset,13     ;add offset in Q28
LDP     #load_ib
SACH    load_ib,3        ;Convert final result to Q15

```

```

;=====  

; conversion of newest a-phase voltage  

;=====  


```

```

POINT_PF2
LACC    ADC_RESULT2, 6
XOR     #8000h
LDP     #templ
SACL    templ
LT      ua_gain           ;ua_gain in Q13
MPY     templ            ;Q13 x Q15 = Q28
PAC
ADD     ua_offset,13     ;add offset in Q28
LDP     #vltg_a
SACH    vltg_a,3        ;Convert final result to Q15

```

```

;=====  

; conversion of newest b-phase voltage  

;=====  


```

```

POINT_PF2
LACC    ADC_RESULT3, 6
XOR     #8000h
LDP     #templ
SACL    templ
LT      ub_gain           ;ub_gain in Q13
MPY     templ            ;Q13 x Q15 = Q28
PAC
ADD     ub_offset,13     ;add offset in Q28
LDP     #vltg_b
SACH    vltg_b,3        ;Convert final result to Q15

```

```
; conversion of output current from active filter
```

```
POINT_PF2
```

```
LACC      ADC_RESULT4, 6
XOR       #8000h
LDP       #templ
SACL      templ
LT        cmpa_gain      ;Ia_gain in Q13
MPY       templ          ;Q13 x Q15 = Q28
PAC
ADD       cmpa_offset,13 ;add offset in Q28
NEG
LDP       #cmp_ia
SACH      cmp_ia,3       ;Convert final result to Q15
```

```
POINT_PF2
```

```
LACC      ADC_RESULT5, 6
XOR       #8000h
LDP       #templ
SACL      templ
LT        cmpb_gain      ;Ib_gain in Q13
MPY       templ          ;Q13 x Q15 = Q28
PAC
ADD       cmpb_offset,13 ;add offset in Q28
NEG
LDP       #cmp_ib
LDP       #cmp_ia      ;calculate cmp_ic
LACC      cmp_ia      ;cmp_ic=-(cmp_ia+cmp_ib)
LDP       #cmp_ib
ADD       cmp_ib
NEG
LDP       #cmp_ic
SACL      cmp_ic
```

```
;-----
; COMPUTE FUNDAMENTAL COMPONENTS
;-----
```

```
Fund  vltg_a, w_coefa, fund_comp_a
Fund  vltg_b, w_coefb, fund_comp_b
LDP   #fund_comp_a
LACC  fund_comp_a
LDP   #fund_comp_b
ADD   fund_comp_b
NEG
LDP   #fund_comp_c
SACL  fund_comp_c
```

```
-----  
;COMPUTE HARMONIC CURRENT FOR A-PHASE  
-----
```

```
LDP      #load_ia  
LACC     load_ia, 16  
LDP      #fund_comp_a  
SUB      fund_comp_a,16  
SACH     err_a
```

```
-----  
;COMPUTE HARMONIC CURRENT FOR B-PHASE  
-----
```

```
LDP      #load_ib  
LACC     load_ib, 16  
LDP      #fund_comp_b  
SUB      fund_comp_b,16  
SACH     err_b
```

```
-----  
;COMPUTE HARMONICS CURRENT FOR C-PHASE  
-----
```

```
LDP      #err_a  
LACC     err_a  
LDP      #err_b  
ADD      err_b  
NEG  
LDP      #err_c  
SACL     err_c
```

```
-----  
;PWM SWITCHING SIGNAL GENERATION  
-----
```

```
LDP      #cmp_ia  
LACC     cmp_ia,16  
LDP      #err_a  
SUB      err_a,16  
BCND     Bphase, EQ  
BCND     Grta,GT  
POINT_EV  
LACC     ACTR  
AND      #1111111111111100b      ;open 1btm switch  
SACL     ACTR  
delay  
OR       #0000000000001100b      ;close 1top switch  
SACL     ACTR  
B        Bphase  
  
Grta    POINT_EV  
LACC     ACTR
```

```

AND      #1111111111110011b      ;open 1top switch
SACL     ACTR
delay
OR       #0000000000000011b      ;close 1btm switch
SACL     ACTR

Bphase
LDP      #cmp_ib
LACC     cmp_ib,16
LDP      #err_b
SUB      err_b,16
BCND     Cphase, EQ
BCND     Grtb,GT
POINT_EV
LACC     ACTR
AND      #1111111111001111b      ;open 2btm switch
SACL     ACTR
delay
OR       #0000000011000000b      ;close 2top switch
SACL     ACTR
B        Cphase
Grtb    POINT_EV
LACC     ACTR
AND      #1111111100111111b      ;open 2top switch
SACL     ACTR
delay
OR       #0000000000110000b      ;close 2btm switch
SACL     ACTR

Cphase
LDP      #cmp_ic
LACC     cmp_ic,16
LDP      #err_c
SUB      err_c,16
BCND     WW, EQ
BCND     Grtc,GT
POINT_EV
LACC     ACTR
AND      #1111110011111111b      ;open 3btm switch
SACL     ACTR
delay
OR       #0000110000000000b      ;close 3top switch
SACL     ACTR
B        WW
Grtc    POINT_EV
LACC     ACTR
AND      #1111001111111111b      ;open 3top switch

```

```

SACL      ACTR
delay
OR        #0000001100000000b      ;close 3btm switch
SACL      ACTR

WW
;-----
;UPDATE COEFFICIENTS
;-----
LDP      #err_a
LT       err_a
LACC     #mio_a
LDP      #templ
SACL     templ
MPY      templ      ;Q15xQ15=Q30
PAC
RPT      #1          ;ue Q15
SFL      ;2ue Q15
LDP      #mio_err_a
SACH     mio_err_a   ;2ue, Q15
LAR      AR2, #w_coeffa
LAR      AR3, #vltg_a
SPM      1
.loop    P_num
MAR      *, AR3
LDP      #mio_err_a   ;2ue*X
LT       mio_err_a
LDP      #vltg_a
MPY      *+, AR2      ;Q30
PAC
LDP      #w_coeffa
ADD      *,16         ;W(k+1)=W(k)+2ue*X
SACH     *+
.endloop
SPM      0

;-----
;UPDATE WEIGHTS
;-----
LDP      #err_b
LT       err_b
LACC     #mio_b
LDP      #templ
SACL     templ
MPY      templ
PAC
RPT      #1
SFL

```

```

LDP      #mio_err_b
SACH     mio_err_b
LAR      AR2, #w_coeffb
LAR      AR3, #vltg_b
SPM      1
loop     P_num
MAR      *, AR3
LDP      #mio_err_b
LT       mio_err_b
LDP      #vltg_b
MPY      *+, AR2
PAC
LDP      #w_coeffb
ADD      *,16
SACH     *+
.endloop
SPM      0

LDP      #dlog_iptr1
SPLK     #load_ia, dlog_iptr1
SPLK     #fund_comp_a, dlog_iptr2
SPLK     #0100h,trig_value ;Trigger value
CALL     DATA_LOG
POINT_PF2
SPLK     #0110000000000000b,ADCL_CNTL2 ;Reset + SOC SEQ1
                                           ;start next ADC

```

```

;~~~~~
;Context restore
;~~~~~

```

```

POINT_PG0
MAR      *, AR7 ;make stack pointer active
LACL     *- ;Restore Acc low
ADDH     *- ;Restore Acc high
LST      #0, *- ;load ST0
LST      #1, *- ;load ST1
CLRC     INTM
CLRC     SXM
RET

```